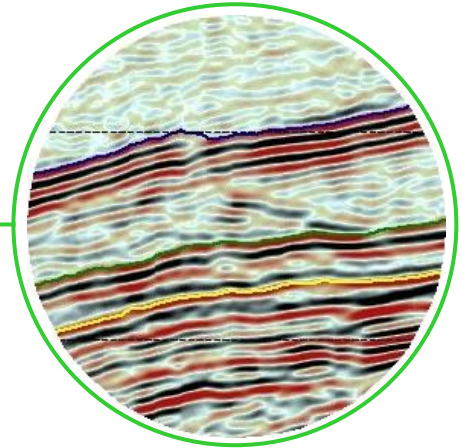


**2011 ADANI
2D SEISMIC SURVEY
Galilee Basin, QLD**



FINAL REPORT

- Interpretation & Data Processing Report

Prepared for

Adani Mining

by

Velseis Processing Pty Ltd

Integrated Seismic Technologies



Prepared for	:	Adani Mining
Prepared by	:	K. McClintock
Endorsed by	:	Velseis Processing Pty. Ltd.
Report No.	:	VP12-580
Date	:	16 January 2012

Velseis Processing Pty Ltd

Integrated Seismic Technologies

Velseis House, 83 Jijaws Street, Sumner Park, Qld. 4074

P.O. Box 118, Sumner Park, Qld. 4074, Australia

Phone: (617) 3376 5544 **Fax:** (617) 3376 6939

Email: processing@velseis.com.au

ABN 30 058 427 204



CONTENTS

INTRODUCTION	3
ACQUISITION	5
Field Parameters	5
Line Summary	5
Survey Information	5
PROCESSING	6
Processing System	6
Data Quality	6
Frequency Content	8
INTERPRETATION	9
Introduction	9
Interpretation Workflow	9
Synthetic Seismogram Generation	10
Picking Horizons	11
Horizon Ties and Depth Conversions	12
Fault Interpretation	16
Fault Resolution	16
Seam Faulting and Structure Summary	19
Stratigraphy Changes	22
CONCLUSIONS AND RECOMMENDATIONS	24
Disclaimer	25
APPENDIX A SEISMIC SECTIONS	26
APPENDIX B FAULT METHODOLOGY	35
APPENDIX C PROCESSING	36
Processing Workflow	36
PROCESSING SYSTEM	38
Parameter Testing	38

Processing Parameters	39
Quality Control	42
Archive	42

APPENDIX D RESOLUTION OF SEISMIC INTERPRETATION	43
---	----

APPENDIX E GLOSSARY	45
---------------------	----

FIGURES

Figure 1. 2011 Adani 2D Seismic Line Layout.	4
Figure 2: Line 2011-07 Raw record SP 300	7
Figure 3: Section data quality Line 2011-07	7
Figure 4 : Spectral Analysis of Line 2011-07, Migrated Stack with spectral enhancement.	8
Figure 5. Synthetic Seismograms.	10
Figure 6. Portion of line 2011-07 illustrating horizons mapping.	11
Figure 7. D1 Roof Two Way Time Horizon (10 ms contours).	13
Figure 8. D1 Roof Gridded Average Velocity (50 m/s contours).	14
Figure 9. D1 Roof Elevation AHD (contour interval 20m).	15
Figure 10. Style and Displacement Histograms	18
Figure 11. Interpreted section line 2011-10	19
Figure 12. Interpreted section line 2011-06	20
Figure 13. Interpreted Seismic Basemap of AB1 seam	21
Figure 14. Line 2011-02 AB1 – AB3 seam interburden thickness change.	22
Figure 15. AB1 to AB3 seam Isopach Map (4m contours).	23

TABLES

Table 1. Field Acquisition Parameters	5
Table 2. Line Summary	5

INTRODUCTION

During October 2011, Velseis Pty Ltd acquired approximately 28.8 km of 2D Enviro-Vib data for Adani Mining. These data, consisting of 9 lines (Figure 1), were acquired within the Adani area in the Galilee Basin approximately 160Km north-west of Claremont.

Velseis Processing Pty Ltd processed these data in November 2011 with the interpretation completed in December 2011.

The main purpose for the survey is to locate faults and other features, associated with the roof of the AB1, AB3, and D1 seams that might influence future mine planning and design.

Products produced for Adani Mining include:

- Interpretation & Processing Report (including acquisition parameters).
- 1:20,000 scaled map of the survey area showing fault geometry and other important seismic anomalies for the Roof AB1 and Roof D1 seams.
- DVD including the folders:

Report: PDF file of interpretation & processing report.

Images: JPEG image files including

- 1:20,000 scaled maps of the location of Roof AB1 and Roof D1 seam faulting.
- 1:5,000 scaled interpreted images of the 9 seismic sections

Faults: DXF & Spreadsheet detailing fault displacements on all seams listed above.

Elevations: Spreadsheet detailing the elevation (AHD) for all seams listed above.

SEGY: Data files for the 2011 2D seismic survey – unfiltered final, unfiltered migrated, filtered migrated and filtered migrated with tvdafd (spectral balancing).

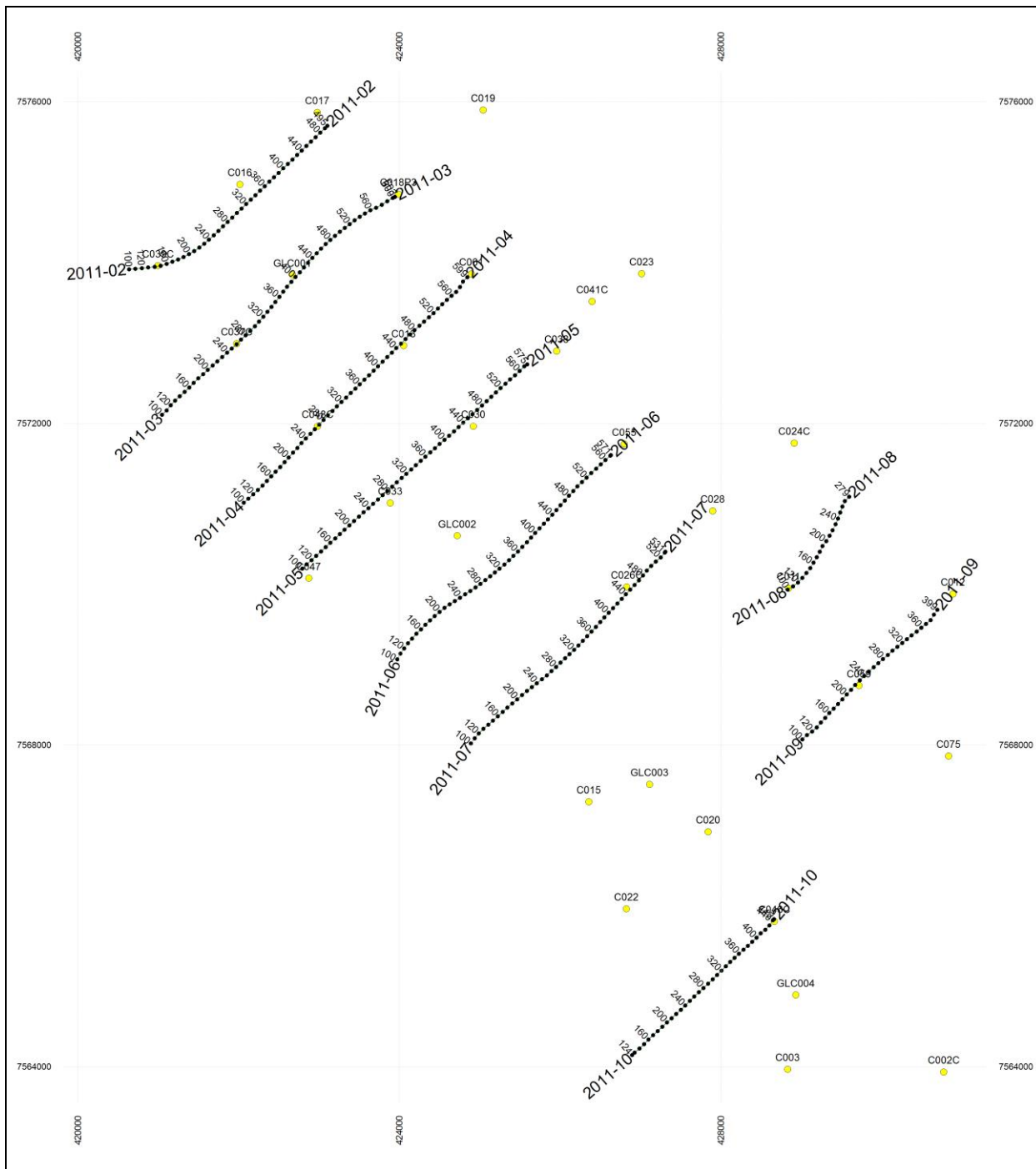


Figure 1. 2011 Adani 2D Seismic Line Layout.

Illustrated are the seismic lines in black and borehole locations black and yellow.

ACQUISITION

Acquisition parameters for the seismic lines discussed in this report are listed in Table 1. The parameters were designed to have maximum offsets tuned to the depth of the target coal seam. The line summary is set out in Table 2.

Field Parameters

Section	Item	Specification
Instrumentation	Instrument	Sercel SN 408
	Recording format	SEG-Y
	Source	IVI Envirovibe 12000, centred between pegs
	Geophone	Sensor Sm-7, 30 Hz 370 Ohm
Parameters	Record length	1000ms
	Sample interval	0.5 ms
	Geophones	3 geophones over 2m, centred on peg
	No. of Channels	240
	Spread	Split spread
	Sweep	20-190 Hz
	No. of Sweeps	1
	Sweep Length	8 sec
	Receiver Interval	8 m
	Shot Point Interval	8 m
	Near Offset	4 m
	Far Offset	956 m
	CDP Fold (nom)	120

Table 1. Field Acquisition Parameters

Line Summary

Line	Station Range	Station Interval (m)	Line length (km)
2011-02	100-496	8	3.17
2011-03	100-604	8	4.03
2011-04	100-600	8	4.00
2011-05	100-576	8	3.81
2011-06	100-572	8	3.78
2011-07	100-532	8	3.46
2011-08	100-280	8	1.44
2011-09	100-400	8	2.40
2011-10	100-443	8	2.74
Total Length			28.83

Table 2. Line Summary

Survey Information

Datum: GDA 94
System: MGA94 Zone 55

PROCESSING

Processing System

The data were processed by Velseis Processing Pty Ltd located in Brisbane, Australia during November 2011.

Velseis Processing uses ProMAX processing software. This is an interactive processing system allowing the user to view data processing at each stage, producing a final result of the highest quality.

The software executes on Velseis Processing's Linux cluster technology. The 262 CPU cluster is configured with minimum dual AMD 1.8-3.2 GHz chips, 2-16 Gbyte memory communicating via a 1 Gbit network and provides significant improvements in processing speed. User interface is via X terminals networked to the main system. Each terminal has a high definition monitor to enable accurate representation of the digital data in pixel form.

Processing Workflow, Processing Parameters and other details are contained in Appendix C.

Data Quality

Data quality observed across the majority of the survey is good with strong and continuous reflections visible. Lines 2011-08 and 2011-09 have a reduced data quality with areas of less prominent reflections.

Figure 2 shows a raw record from line 2011-07 exhibiting strong reflections. Whilst groundroll (linear noise) is also visible, this is easily removed during processing.

The Vibroseis (Enviro-Vib) technique employs a surface energy source to generate the seismic energy (sound waves). Two of the advantages of this technique are the acquisition of high fold data without expensive shot hole drilling, and a low level of environmental impact. The disadvantages are similar to those of any surface energy source method. Specifically, the data quality may be susceptible to adverse surface and near-surface conditions (i.e. deep, variable weathering, and surface basalt cover).

For the 2011 Adani survey, a deep Tertiary cover is known to exist and observed in the raw records and on the final stacked images (Figure 3). In this instance this Tertiary cover has not negatively impacted on the interpretation of these data.

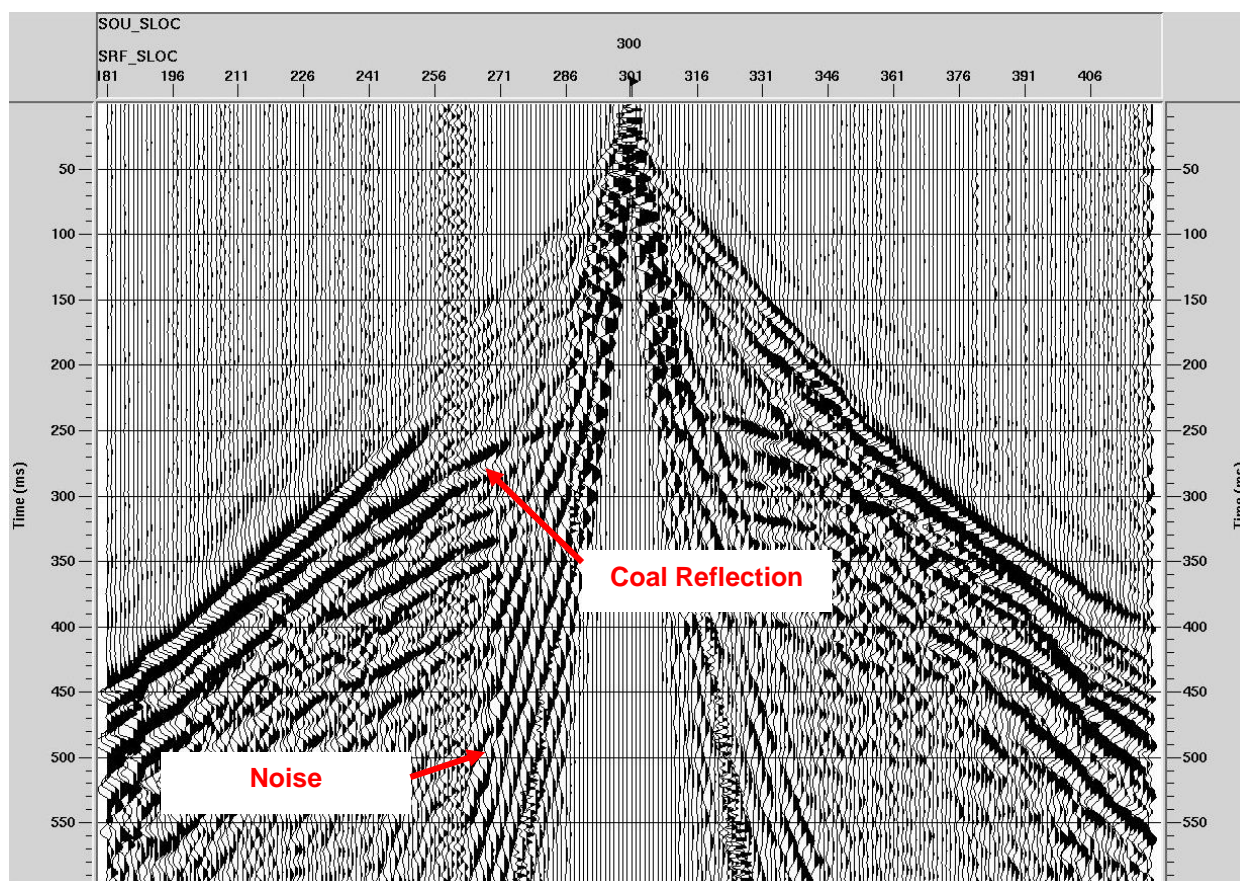


Figure 2. Line 2011-07 Raw record SP 300

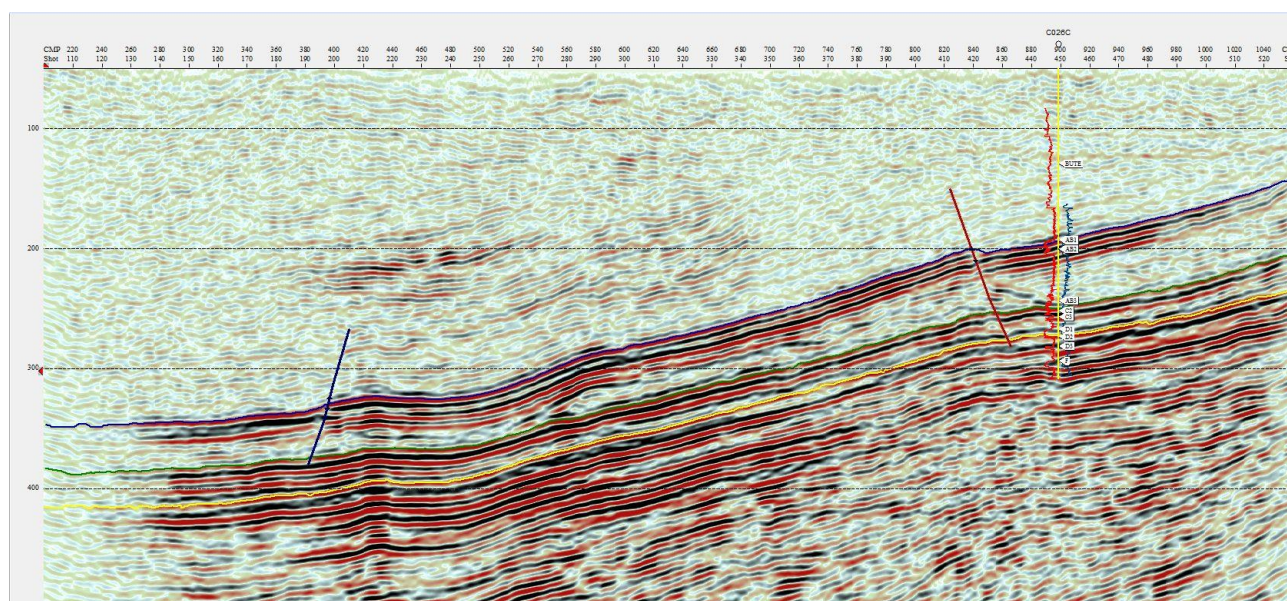


Figure 3. Section data quality Line 2011-07

Frequency Content

In addition to evaluating the signal to noise of the raw record data quality, frequency spectra may be used to examine the frequency content (temporal resolution) of these data. Frequency spectra (plot of the seismic frequency versus the power of that frequency contained within the data) provide a simple graphical illustration of the frequency bandwidth of the data and may be used to determine the resolution of the seismic dataset.

The vertical resolution of any seismic dataset influences the ability to detect and characterise subtle changes in structure and stratigraphy. Vertical resolution is determined by both the datasets bandwidth and dominant frequency. By using Figure 4, the bandwidth and dominant frequency for these data may be determined. This is best achieved by examining the F-X plots, which plot the frequency content on a trace-by-trace basis (bottom left hand plot of Figure 4). On this plot, reflection energy is displayed as high amplitude coherent data, with the noise indicated by the low amplitude or random energy. Figure 4 shows the spectra for Line 2011-07 and indicates that these data exhibit a maximum frequency of 160Hz and a dominant bandwidth of between 40-150Hz. When compared to other surface based surveys targeting shallow coal seams, the frequency characteristics of these data can be considered extremely good. The high dominant frequency and broad bandwidth suggest that the resolving power (Appendix D) of these seismic data is very good.

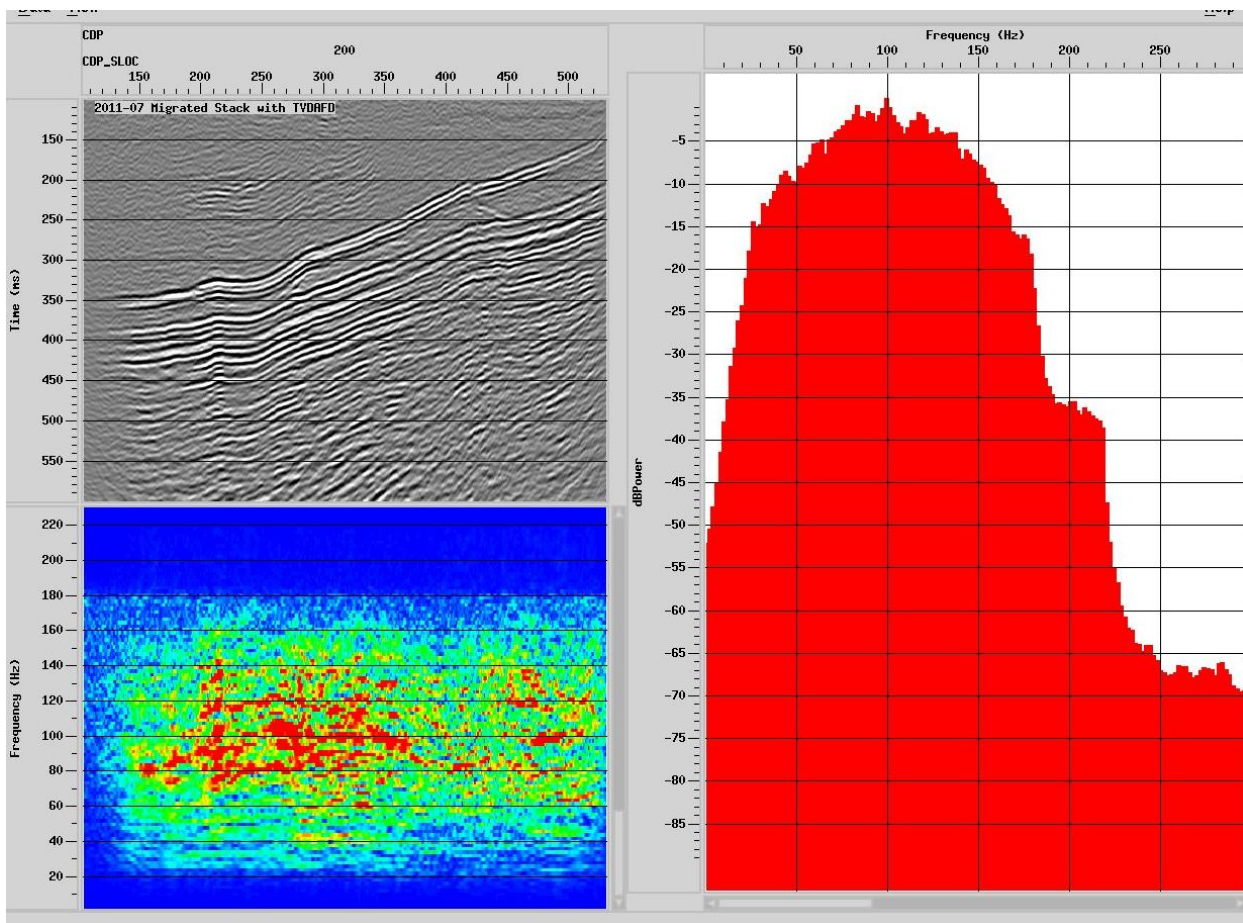


Figure 4. Spectral Analysis of Line 2011-07, Migrated Stack with spectral enhancement.

INTERPRETATION

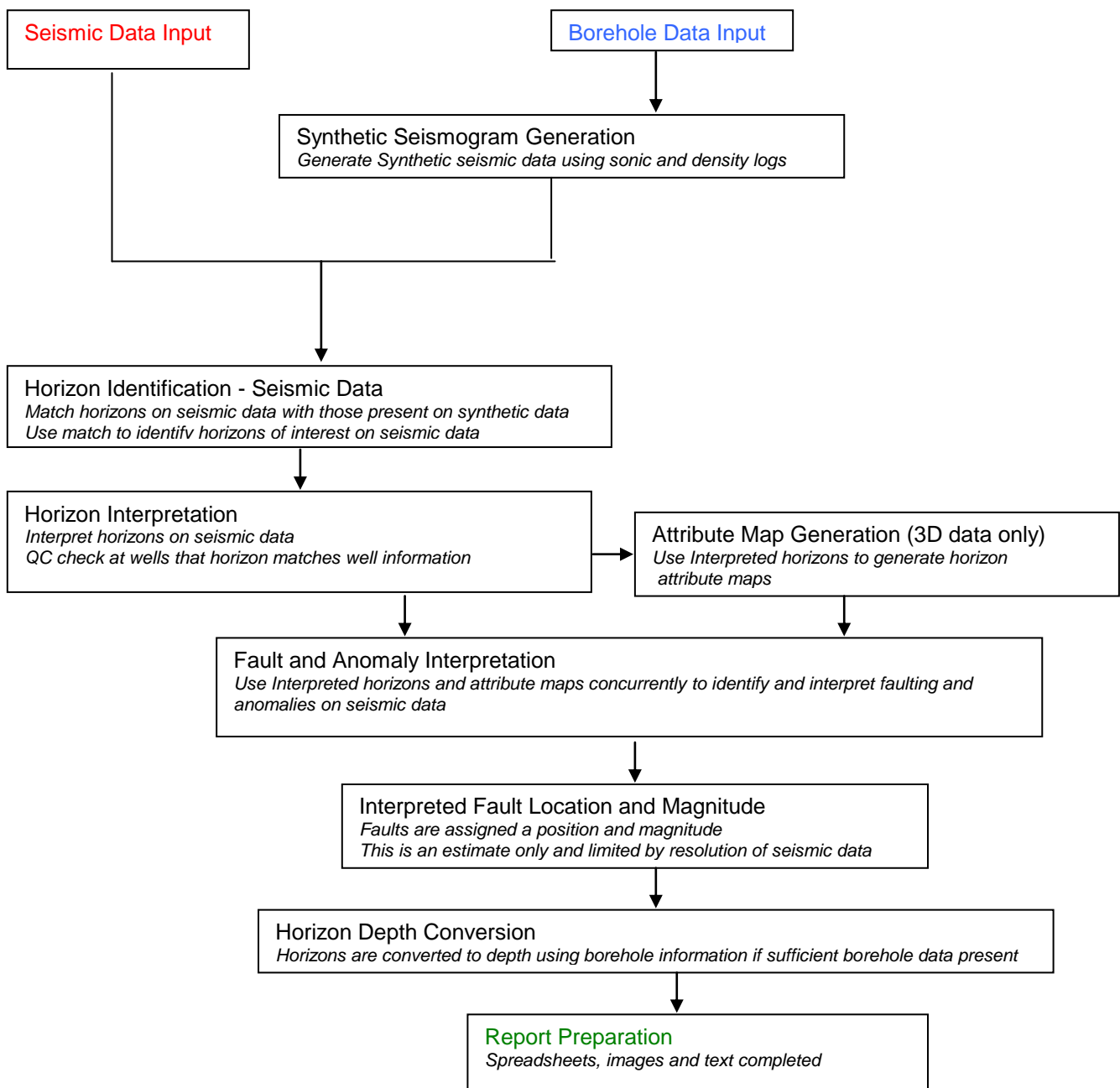
Introduction

These data were interpreted at Velseis Processing's offices in Brisbane during December 2011. Interpretation was conducted on a PC using the 'SeisVision' program.

An outline of the interpretation workflow is presented in the following section. All borehole collars and seam-pick data, as well as geophysical logging data were provided by Adani Mining.

It should be noted that for the purposes of interpretation, a number of different processed seismic data sets were evaluated to determine which gave the most coherent and continuous response for the interpreted seam horizons. Data versions evaluated included final, migrated, and migrated with true amplitude spectral extension applied. From this evaluation, it was determined that the migrated with spectral extension provided superior resolution for the target horizons.

Interpretation Workflow



Synthetic Seismogram Generation

To assist the interpretation, Adani Mining provided geophysical logs and seam picks for boreholes within the 2D survey area. These were provided to link the seismic reflectors to the local geology, which is achieved via the generation of synthetic seismograms.

$$R = \frac{\rho_2 v_2 - \rho_1 v_1}{\rho_2 v_2 + \rho_1 v_1}$$

R = Reflection coefficient
 ρ = Density
 v = Velocity

The reflection coefficient is directly related to the contrast in acoustic properties across the interface. The time corresponding to each coefficient is calculated by integrating the sonic log. The reflectivity series is then convolved with a defined wavelet to generate the synthetic trace. The synthetic seismogram (time series) can then be directly correlated with the wireline log to identify geological boundaries.

Figure 5 illustrates this process for borehole C026C, located close to Line 2011-07. To tie the seismic character of the synthetic to the actual 2D seismic data, a frequency of 90 Hz is used with a phase shift of 180 degrees. Overall the seismic character match between the synthetic and seismic data is excellent, which provides confidence in accurately associating the various seams to reflection horizons. The horizons selected for mapping are shown on Figure 5 as the AB1 (blue), AB3 (green), and D1 (yellow) seams.

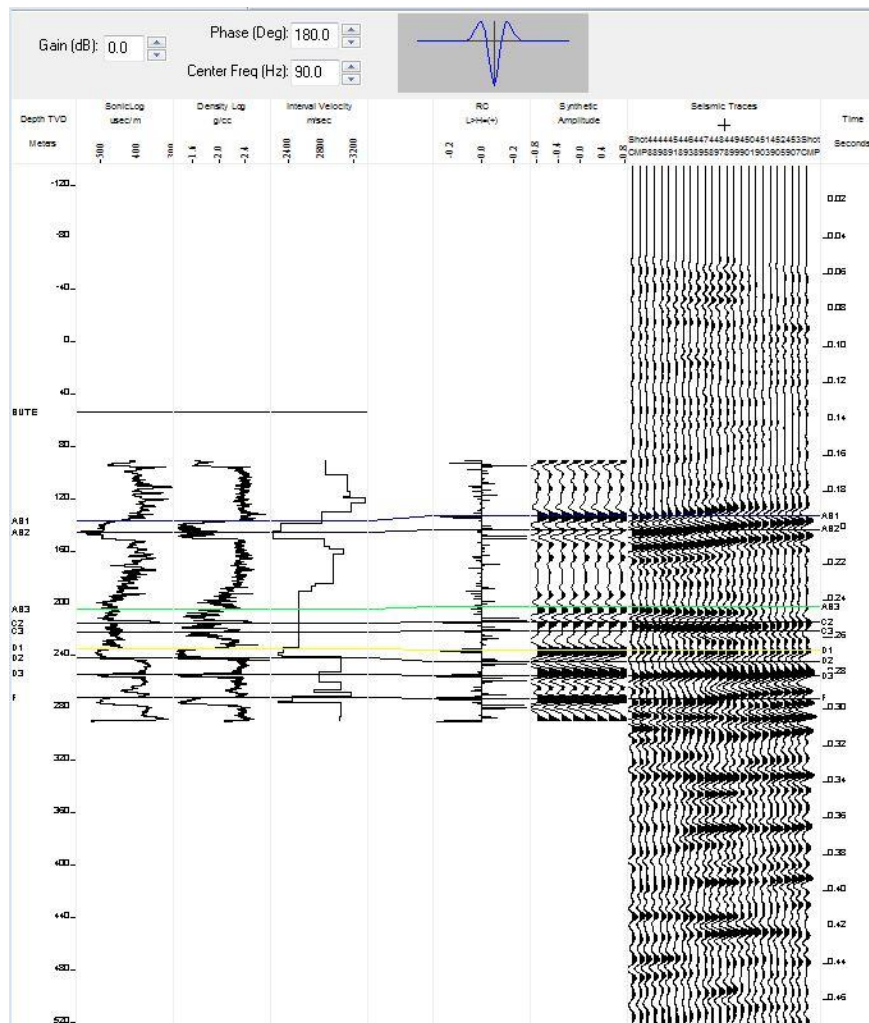


Figure 5. Synthetic Seismograms.
 Borehole C026C located on line 2011-07.
 Seams shown are AB1 (blue), AB3 (green), and D1 (yellow) seams.

Picking Horizons

The interpretation scope of work supplied by Adani Mining requested that, if possible, a number of target coal seams should be identified and mapped throughout the 2D survey area. Seams AB1, AB3 and D1 were mapped during this interpretation. In a geological context, a single seam may be constructed from a number of coal seam plys. For example, the AB3 seam is broken into plys ranging from AB3 to AB33. For the purpose of this interpretation, horizons mapped across the entire area are in all cases the upper most ply.

With the aid of synthetic seismograms (Figure 5), the roof of the specified seams have been mapped to the trough of the corresponding seismic reflection event. Figure 6 illustrates this horizon mapping for a portion of line 2011-07 centred on borehole C026C (Figure 5).

Overall the reflection horizon continuity is excellent and where present, the majority of the target seams AB1, AB3 and D1, can be mapped with confidence across the majority of the lines. There are however exceptions to this, and these are as follows. Horizons on line 2011-08 were unable to be picked due to poor data quality. Also, as the coal seam stratigraphy gradually shallows from west to east, the target seams sub-crop against the Tertiary boundary, which limits the extent of the target horizons.

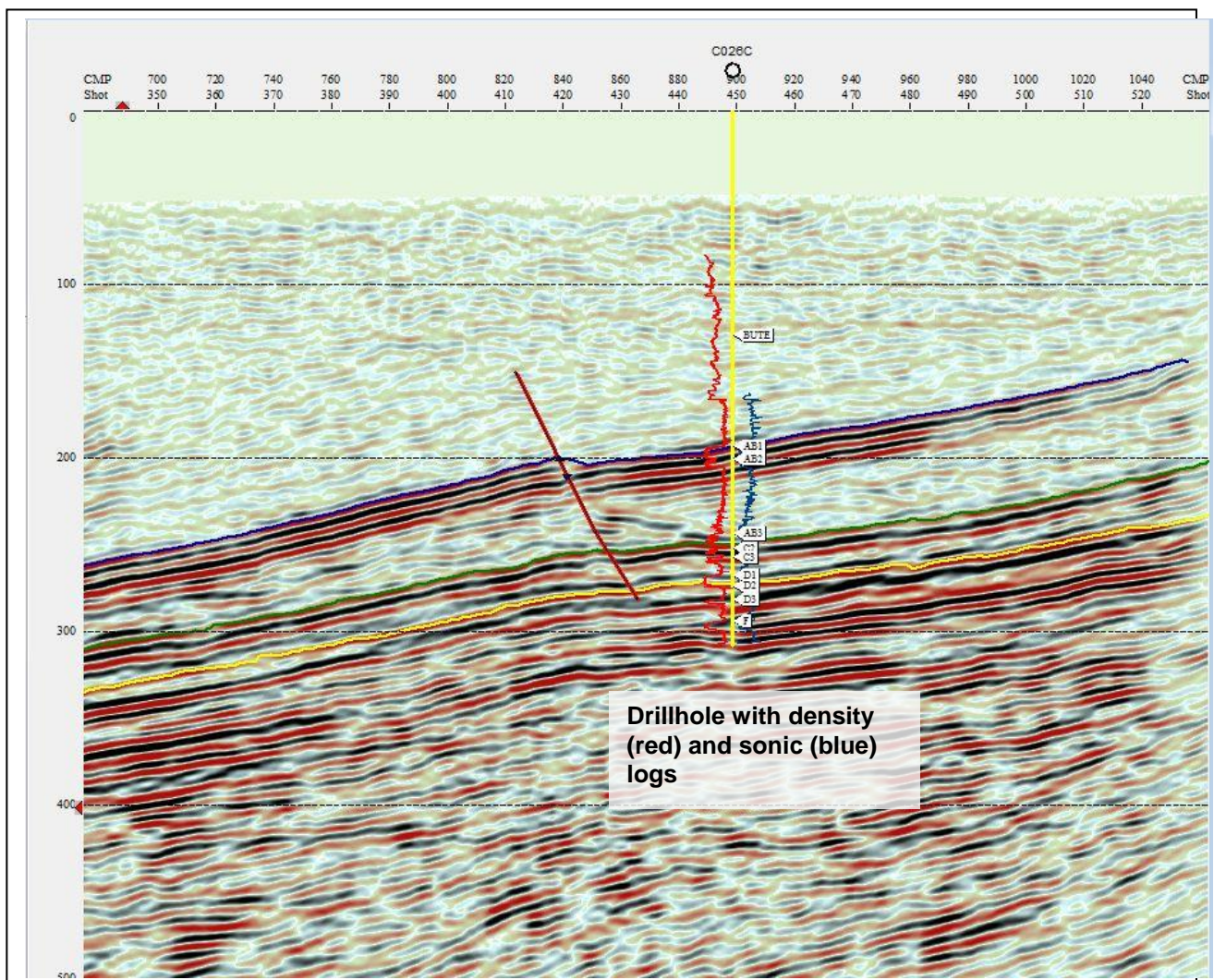


Figure 6. Portion of line 2011-07 illustrating horizon mapping.

Seams shown are AB1 (blue), AB3 (green), and D1 (yellow) seams. The location of the borehole, used in the synthetic seismogram (Figure 5), is shown with the geophysical logs and seam picks. Various styles of faulting are picked and are coloured with respect to the interpretation confidence, probable=red and possible=blue. Orientation looking north-west.

Horizon Ties and Depth Conversions

As all seismic data are measured in Two-Way Time (TWT), it can be difficult to incorporate these mapped time horizons into mine planning packages. To incorporate these effectively the horizons need to be referenced to depth. To do this, the seam picks (depth) and corresponding horizon TWT (Figure 7) maps have been used to produce interval velocity control points for the seams. These interval velocity points are then gridded via a minimum curvature algorithm (Figure 8) and then multiplied by the TWT to produce the D1 seam elevation map (Figure 9).

This procedure has been followed for all seams with the respective seam RL data included in the spreadsheets on the DVD, which accompanies this report. As the deepest of all the target seams studied, the D1 seam is the more laterally extensive and extends almost to the extremities of all lines. For the shallower seams, the provision of elevation data is restricted on the basis of where the shallow seams sub-crop against the Tertiary boundary.

The success of the depth conversion process is dependent upon the number of holes available to control the depth conversion and the degree of geological heterogeneity. Whilst the relative (localised) seam level changes can be considered reliable, the absolute values of elevation should be treated with caution. Despite this, the interpreter feels that while the density of suitable control holes within the vicinity of the seismic lines is low, the uniform appearance of the interval velocity map (Figure 8) suggests that the absolute elevation for the seam roofs can be considered a useful tool for planning purposes.

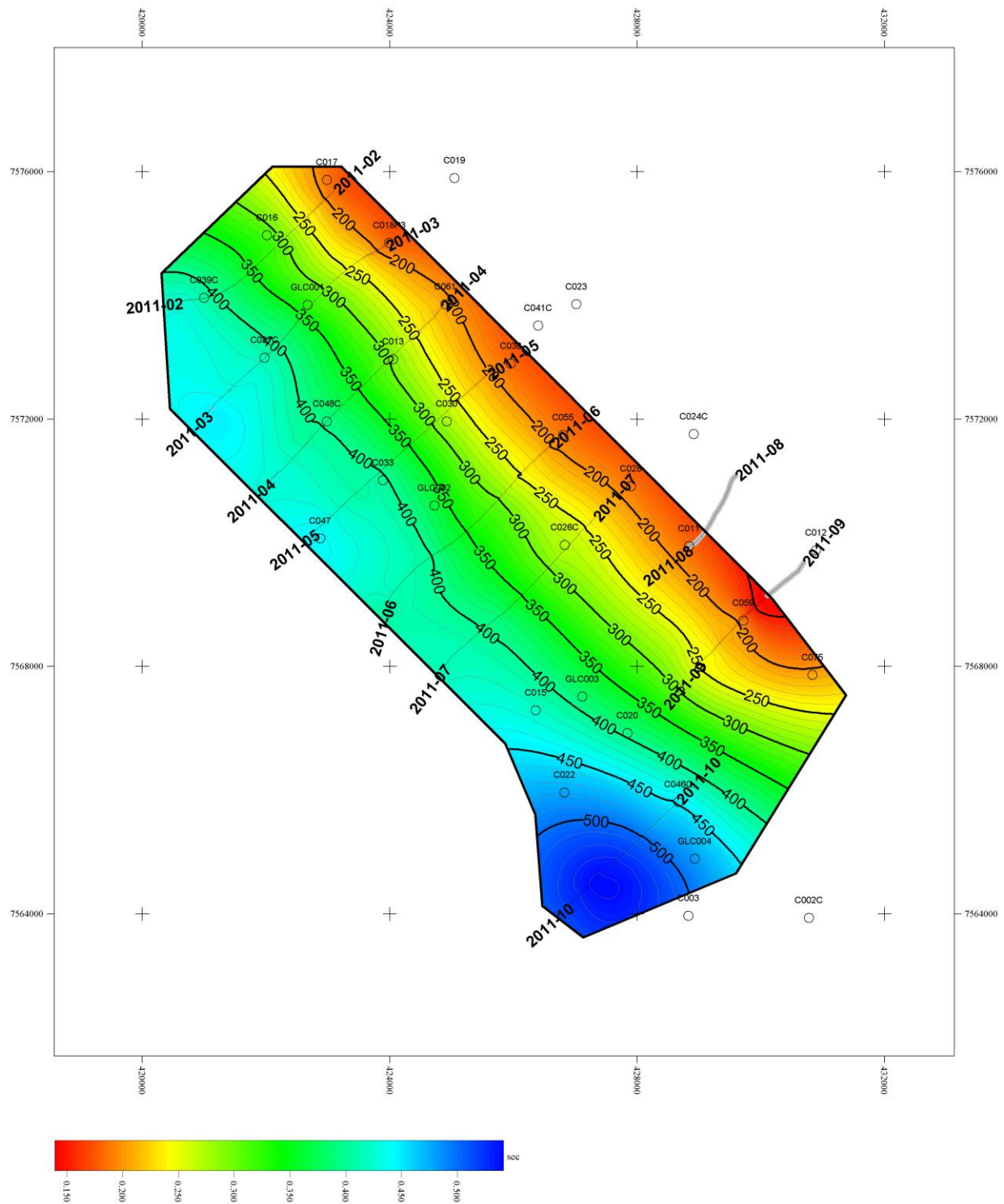


Figure 7. D1 Roof Two Way Time Horizon (10 ms contours).

Note: Two-way time is the time taken for the seismic energy to travel from source (i.e. shot point) to the target reflector and back to the receiver (i.e. surface geophone). Major geological features of the seam are apparent, as well as lineaments that correspond to zones of faulting.

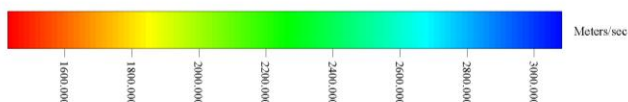


Figure 8. D1 Roof Gridded Average Velocity (50 m/s contours).

Note: This figure represents the velocity for the interval from surface to the roof of the D1. D1 roof picks for suitable drillholes, along with their corresponding D1 horizon pick times were used to calculate the velocity at each borehole, which was then gridded by a minimum curvature algorithm. Gridding honours the horizon pick between boreholes.

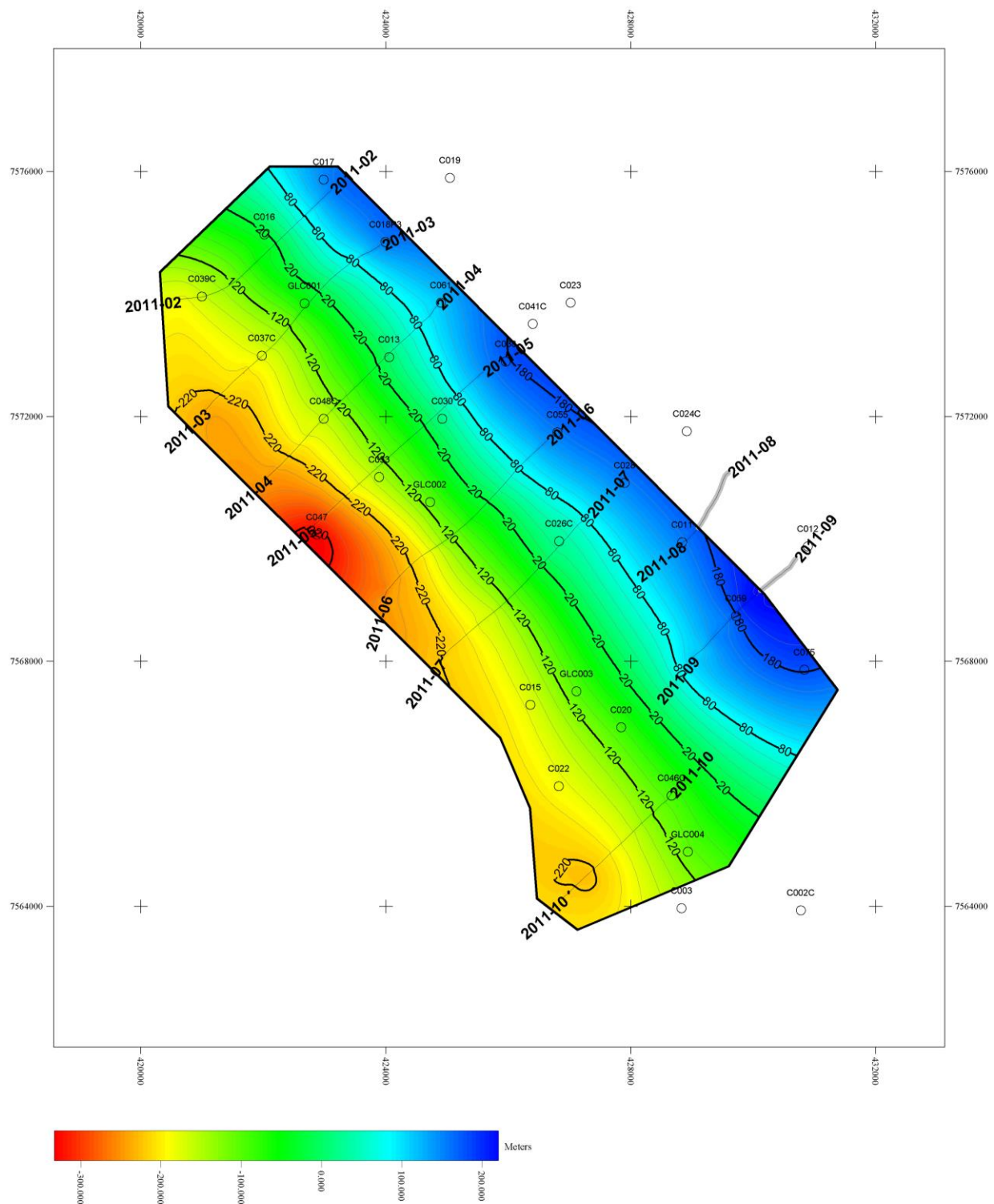


Figure 9. D1 Roof Elevation AHD (contour interval 20m).

Note: This figure represents the depth conversion of the interval velocity point map produced in (Figure 8) by multiplying by the TWT.

Fault Interpretation

N.B. An annotated and scaled copy 1:5000 of each seismic section is included on the DVD accompanying the report. An interpreted image for all the lines (not to scale) is included in Appendix C.

The principle purpose for conducting this seismic survey was to identify faults and other features that are a hindrance to underground mining. A number of such features have been identified on the seismic data. Faults that intersect the AB1, AB3 and D1 seams have been characterised by estimating their location, style, and vertical seismic displacement.

Fault Resolution

It is important to recognise that the resolution of the seismic technique is limited by both frequency and space. Whilst frequency limitations affect the ability to accurately determine coal seam thickness or interburden thickness, it is the spatial limitation that generally hinders fault characterisation.

Consider the following example. Fault A is a single normal fault and has a throw and heave of 6m and 15m respectively. Fault zone B is made up of a series of smaller normal faults with throws measured at 2m and the zone extends over the same distance as in A. Given the limits on spatial resolution, it is likely that both structures would exhibit similar seismic character. Thus, whilst we may be able to measure the net throw across a fault zone, the real geological conditions may be somewhat different. This resolution ambiguity must be taken into account when using this data for coal seam continuity prognoses.

The vertical seismic displacement for each fault is calculated by measuring the change in horizon time over the interpreted fault. This represents a two way time and needs to be halved. A velocity of 2400 m/s was used to convert this time into depth. This velocity has been chosen by both an examination of the sonic data and the velocity maps produced during the depth conversion process.

Vertical seismic displacement = (Change in seam time/2) * 2400

It has **not** been possible to confidently interpret structures exhibiting vertical seismic displacements of **less than 3m**. This limitation relates to the vertical resolution limitations which impacts on the interpreter's ability to confidently distinguish between a subtle structure or a seam roll.

Fault Error Limits

Consideration must be given to the errors in the measurement of both the seismic displacement and structure location. The seismic displacement is the vertical change in depth measured off the seismic data, and depending on the confidence of interpretation may be indicative of faulting. This measurement has an estimated error of +/- 2m. The lateral error in the position of the fault may be in the order of +/- 15m from the true position. These inaccuracies need to be taken into account during mine design, in particular when positioning development roads in the vicinity of any fault.

As indicated, the process of fault characterisation attempts to provide information relating to fault style, position and size. With respect to the estimate of displacement across an interpreted structure, the data provided both on maps and in the DXF files have the error quoted above built in. That is, rather than representing displacement via a single number e.g. 5m, it is represented by a displacement range based on the estimated error e.g. 3-7m.

At present the errors quoted are estimates and have been taken from other 2D survey areas, which have utilised the Vibroseis technique as a seismic source. It may be possible to obtain more site specific errors once the validation drilling programme has been reconciled against the 2D seismic interpretation.

Fault Confidence

Variations in data quality may often result in less confident structural interpretations. Thus structures appearing on all maps have been colour coded to reflect these levels of confidence.

Two levels of interpretation confidence have been described in descending order of confidence.

- Probable/Confident Fault (F) – colour coded red and generally characterised by horizon dislocation, at or above and below the target seam.
- Possible Fault (P) (possible fault, flexure or seam roll) – colour coded blue and characterised by a change in seam gradient but with generally no seam dislocation apparent. May also indicate that interpretation confidence is reduced due to reduced data quality.

Fault Names

The following naming convention has been applied to structure interpreted at all seam levels.

Character 1 may be F or P, which defines the confidence level of interpretation (F = probable fault; P = flexure - roll or possible fault). Character 2 may be N, R, T or U for normal, reverse, thrust or undefined faulting. Characters 3 - 5 is a unique and sequential identifier, commencing at 001.

Fault Characterisation Summary

A detailed list of the fault characterisation for the Adani 2D seismic survey area may be found as an Excel spreadsheet on the DVD accompanying this report. This includes information relating to fault position, estimated vertical seismic displacement, and confidence level. By way of a structural summary, Figure 10 is provided.

Figure 10a represents the distribution of both the interpretation confidence and structural style, whereas Figure 10b illustrates the displacement frequency for all seams regardless of the interpretation confidence.

With respect to the structural style distribution, the survey area does not have many probable interpreted faults and those which are picked are all normal. For the possible structures, there are almost as many reverse as normal faults interpreted. Recall that possible (low confidence) structures often are smaller in scale and due to resolution limitations, are difficult to distinguish between seam rolls. Therefore, many of these possible reverse faults may either be small scale structure or simply seam rolls.

As indicated, Figure 10b is a summary of the probable and possible fault displacements for all seam levels. In this instance the displacements have been grouped into a series of displacement bands (<3m, 3-6m, and 7-9m). As shown, the survey area is dominated by small scale structure/rolls with approximately 95% of all structure exhibiting displacements of less than 6m. For the structures listed as <3m (60%), these are biased towards the low confidence end of interpretation.

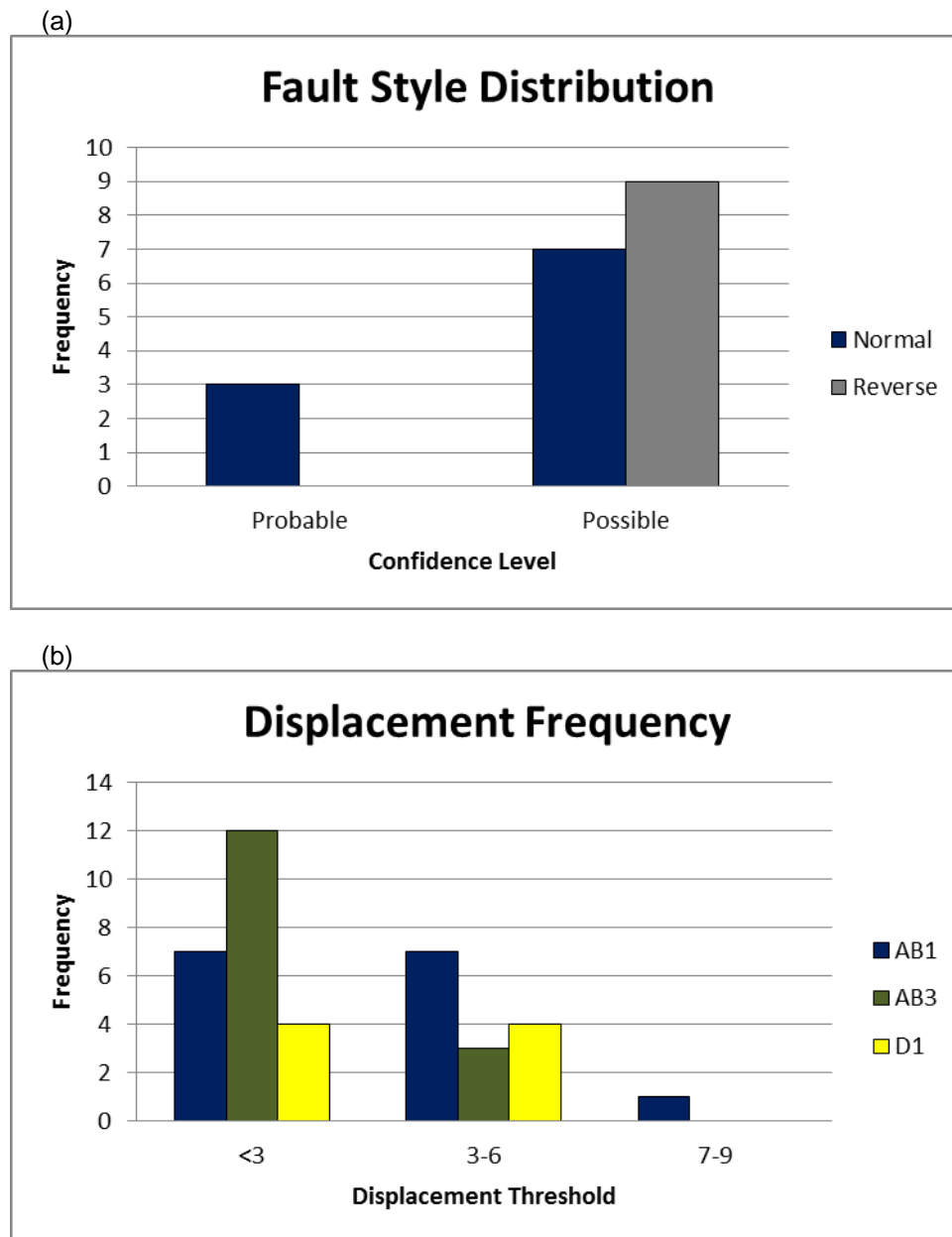


Figure 10. Style and Displacement Histograms
(a) Distribution of fault style and (b) Distribution of displacements.

Seam Faulting and Structure Summary

Within the area of the 2D Seismic Survey, the Coal Measures dip in a general fashion from north-east to south-west.

As outlined above, the overall survey area is not dominated by either style of faults however the probable interpreted faults are all normal (Figure 10a).

Throughout the study area these faults exhibit variable characteristics. Whilst virtually all are high angle, the vertical extent varies significantly.

Figure 11 displays a section indicating a large probable normal fault along with a shallow possible normal fault (FN002 & PN010). The probable fault penetrates the overlying stratigraphy as well as two of the target coal seams. The displacement of the fault diminishes rapidly with the displacement at the AB1 seam interpreted at 6-10m to <3-4.6m in the AB3 seam. PN010 has been interpreted as low confidence, partly due to its small scale but also due to being at the end of the line, only in the AB1 seam with a displacement of <3 – 4.6m which cannot be confidently continued to deeper seams.

Line 2011-06 (Figure 12) shows a greater density of possible faulting than other lines with a series of reverse faults and one normal fault being interpreted. These have different characteristics to the above described fault as they have similar sized displacements from one target seam to the next. This line contributes the most to the count of possible reverse faults seen in Figure 10a with the majority of other possible faults in the survey area being dominated by normal faults.

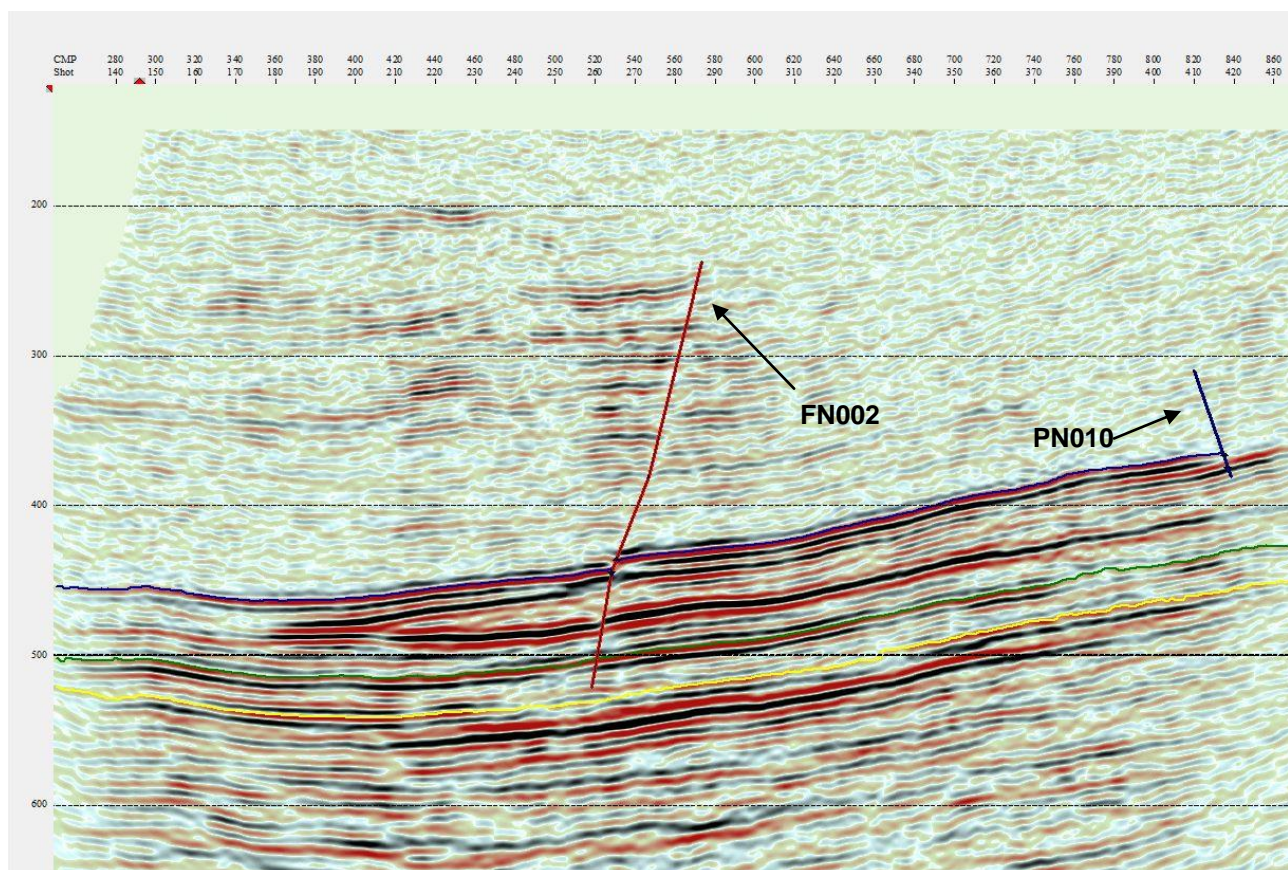


Figure 11. Interpreted section line 2011-10

Seams shown are AB1 (blue), AB3 (green), and D1 (yellow) seams. Various styles of faulting are illustrated and are coloured with respect to the interpretation confidence, probable=red and possible=blue. Orientation looking north-west.

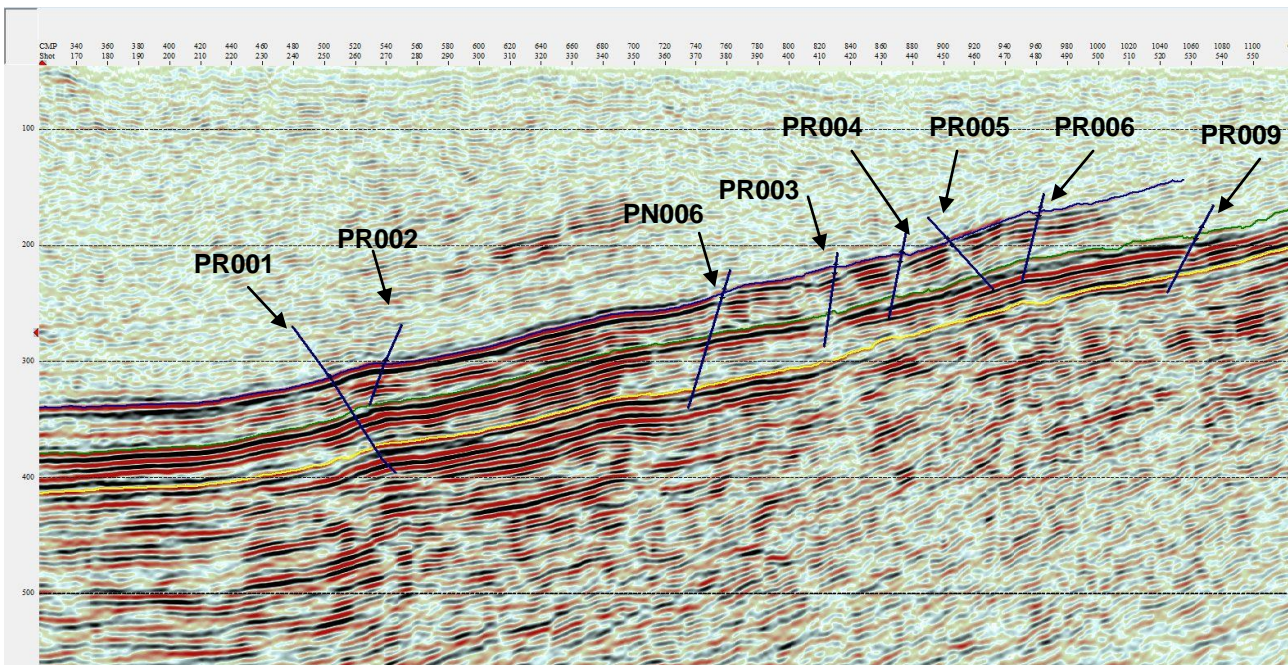


Figure 12. Interpreted section line 2011-06

Seams shown are AB1 (blue), AB3 (green), and D1 (yellow) seams. Various styles of faulting are illustrated and are coloured with respect to the interpretation confidence, probable=red and possible=blue. Orientation looking north-west.

In addition to providing interpretation in vertical section, every effort has been made to interpolate these structures laterally, although, due to the large line separation this lateral interpolation has not been possible.

The interpreted seismic basemap of the AB1 seam (Figure 13), and reproduced at the D1 seam, is a summary of all structural entities. These basemaps also have a number of other entities annotated on it. Most obvious are the seam structure contours (AHD), which provide a guide as to the changing seam grade across the area, along with an orange line which denotes the limit of the seams (AB1 seam only). Scaled images have been provided on the DVD.

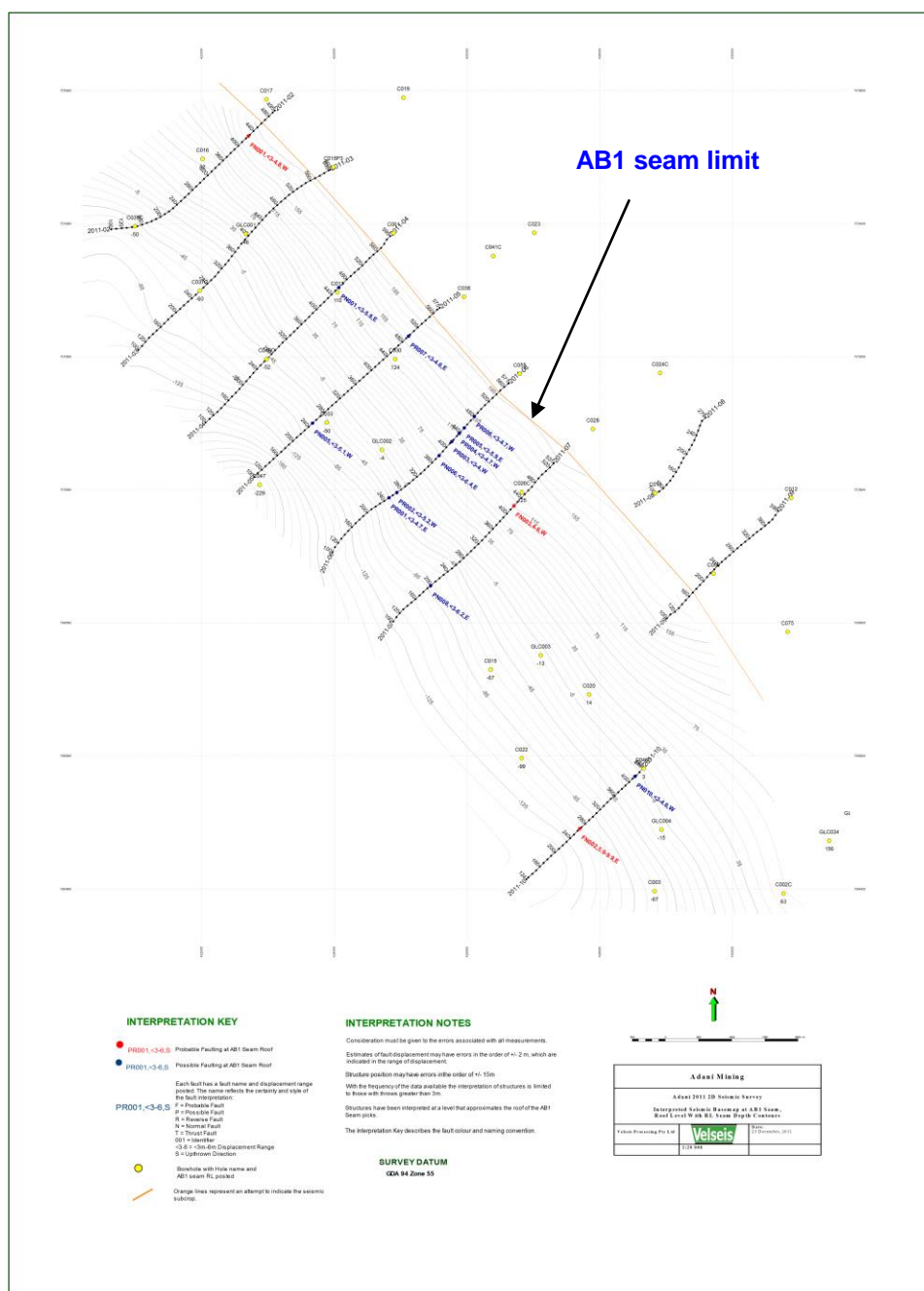


Figure 13. Interpreted Seismic Basemap of AB1 seam

Interpreted seismic basemap for the AB1 seam showing location of probable (red) and possible (blue) interpreted faults, along with seam elevation contours and seam limit in orange.

Stratigraphy Changes

Accurate fault characterisation is still the primary focus for any seismic survey conducted in conjunction with coal mining operations. However, it is also useful to obtain stratigraphic information during the interpretation process. Whilst subtle stratigraphic changes are difficult to detect using widely spaced boreholes and 2D lines, broad scale changes are often easily observed.

During the interpretation of these seismic lines, a significant interburden thickness change between the Roof AB1 and AB3 seams has been noted. This is most likely linked to an obvious stratigraphic structure seen in Lines 2011-02 and 2011-03 (Figure 14) between seams AB1 and AB3 which has been interpreted as a seam split, however which seam is splitting is undetermined. It becomes less apparent in the vertical sections through Lines 2011-03 and beyond. Figure 14 illustrates the observed seismic interburden thickness change in Line 2011-02, indicated by the yellow polygon, along with the seam split shown in the red circle.

Using the depth conversion process highlighted above, the depth converted AB1 and AB3 seam horizon data have been used to generate an AB1 – AB3 seam isopach map (Figure 15). This map is useful as it provides an indication as to the interburden variability for these two seams throughout the study area. As illustrated by Figure 15, this thickness change is gradual with an area of thickening in the north-west and a thinning in the centre of the polygon in the area of lines 2011-05 and 2011-06. Line 2011-06 has a fairly constant thickness across the line. The thickening in the north-west is postulated likely due to the increase of clastic sedimentation associated with the seam split.

Once again the isopach map provided is derived from the depth conversion of widely spaced 2D lines using sparse borehole data. As such, this map provides a relative and not absolute indication for the AB1 to AB3 seam interburden and should be used as a guide only.

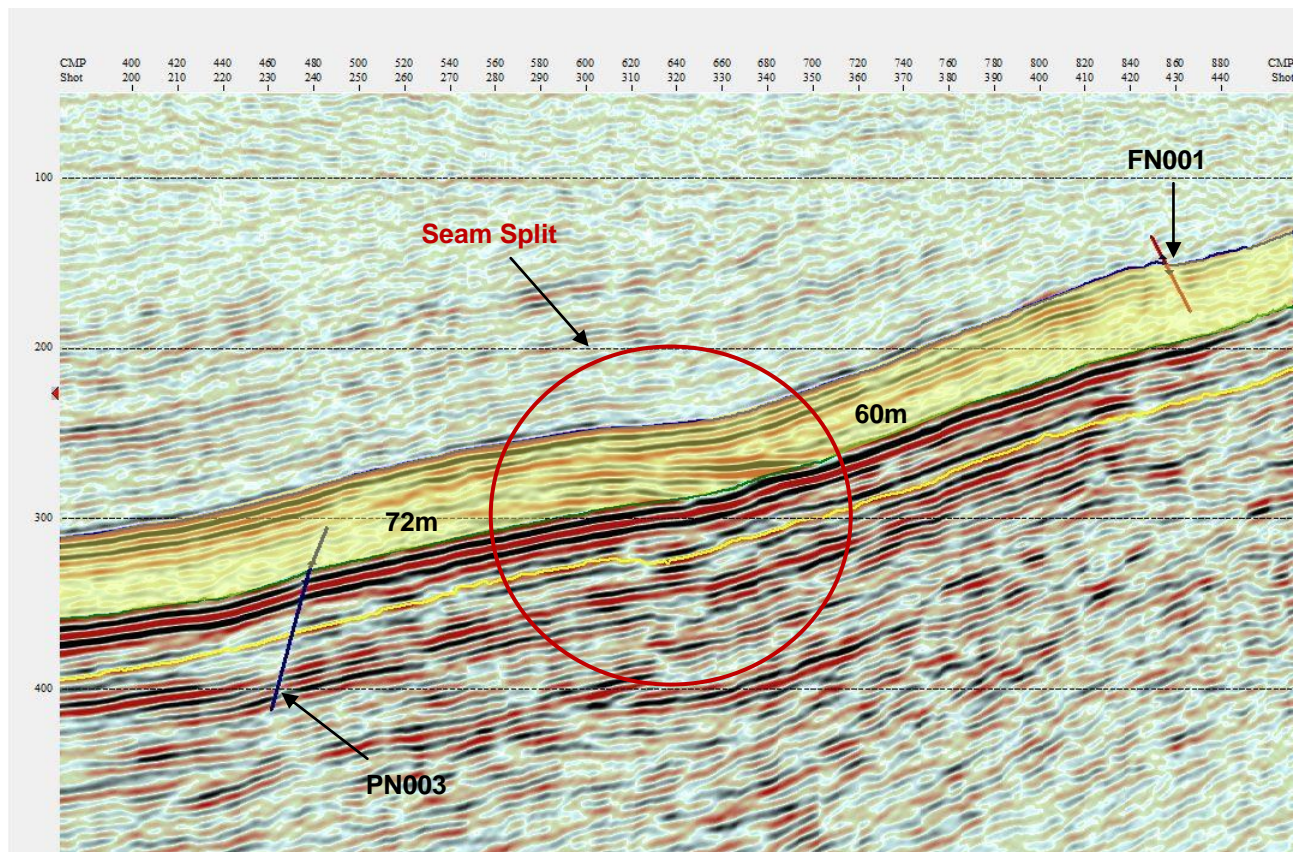


Figure 14. Line 2011-02 AB1 – AB3 seam interburden thickness change.

Seams shown are AB1 (blue), AB3 (green), and D1 (yellow) seams. Various styles of faulting are illustrated and are coloured with respect to the interpretation confidence, probable=red and possible=blue. Interburden thickness change labelled in the yellow polygon. Orientation looking north-west.

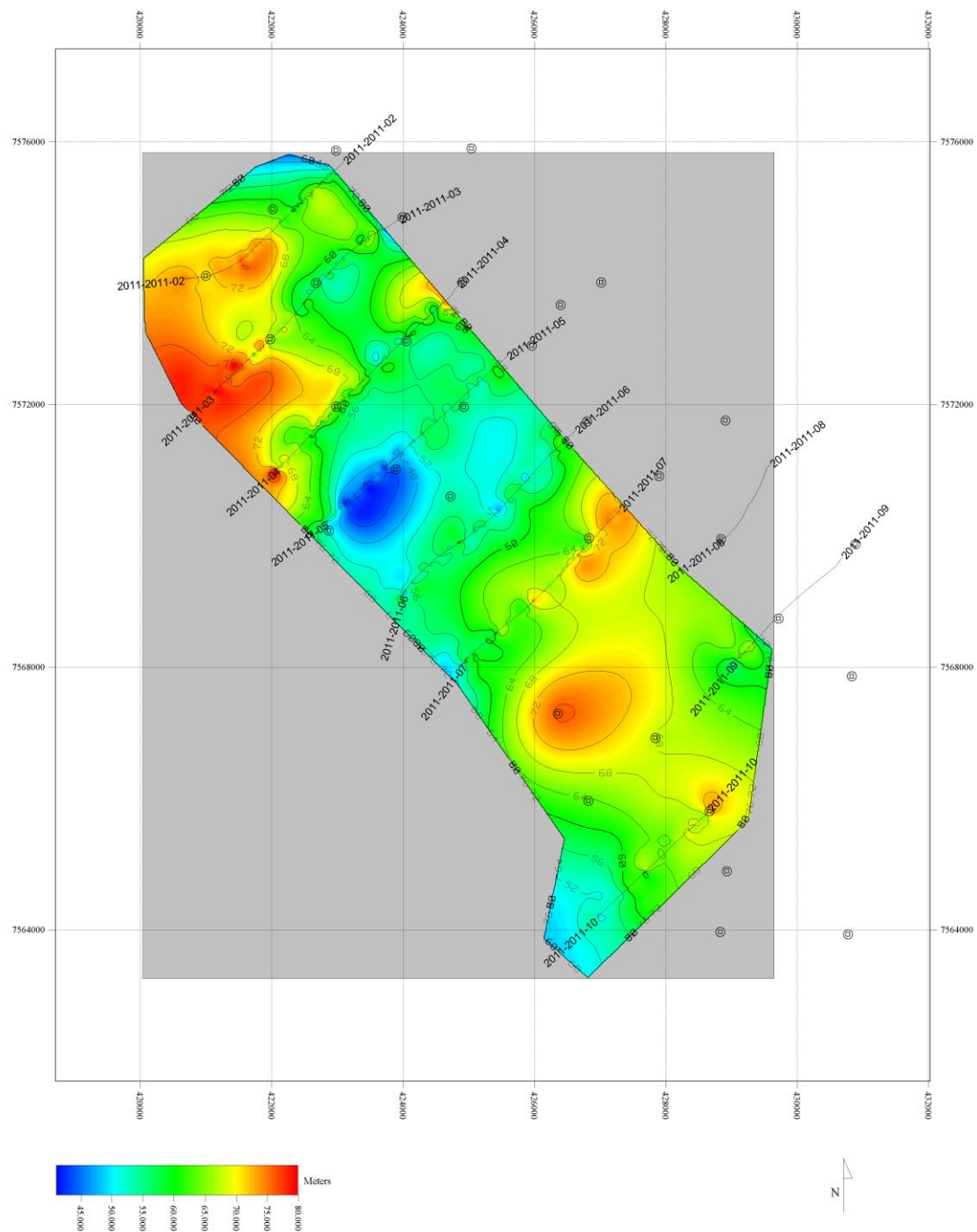


Figure 15. AB1 to AB3 seam Isopach Map (4m contours).

Isopach map of the separation of Roof AB1 and AB3 seams, generated from the depth converted seam horizon data.

CONCLUSIONS AND RECOMMENDATIONS

The 2011 2D Adani Seismic Survey has been successful in providing detailed geological information for use in further exploration and future mine planning.

A number of faults were defined which may prove to be a hindrance to mining operations. An attempt has been made to accurately characterise structures based on position and seismic displacement. The location and geometry of structures as depicted on several different maps and within spreadsheets will provide the basis for a detailed structural analysis of the survey area. Unfortunately due to the large line spacing, it has not been possible to interpolate faults across lines.

In addition to the structural characterisation, all interpreted horizons have been depth converted. Users of this information should acknowledge that this is based on gridding widely spaced 2D data, using sparse boreholes as control. Therefore, these depth converted horizons provide a good indication of the relative changes in seam grade and should be used as a guide only, for determination of seam depth changes.

An attempt has also been made to provide a better understanding of the change in coal seam stratigraphy throughout the survey area. Specifically, the depth converted coal seam horizons have been used to generate an AB1 to AB3 seam interburden thickness map, which shows a gradual thickening to the north-west of the survey area and a thinning in the vicinity of Lines 2011-05 & 2011-06. It has been postulated that this structure is linked to the increase in clastic sedimentation associated with the seam split seen in lines 2011-02 and 2011-03.

The author suggests that a representative set of faults and features be validated against a series of newly acquired holes. Validation drilling of any new seismic dataset is important not only to confirm a representative set of faults and features that have been interpreted from this seismic survey, but also to evaluate the physical measurements (fault displacement and position) and associated errors that result from the interpretation. The results of this validation programme should be reconciled against the current interpretation and if required the interpretation should be modified on the basis of this new geological information.

Additionally, the seam elevation data resulting from these new holes should be reconciled with the seam elevations derived from the seismic depth conversion. By comparing the seam elevation in this manner, an understanding of the errors in the seismic derived elevation for the target seam may be obtained. Following this reconciliation, these new holes should be incorporated into the interpretation database and used as additional control for a revised depth conversion. This iterative approach to seismic depth conversion should be undertaken for any future holes drilled within the survey area.

It is recommended that mine planning staff adopt a pro-active approach to integrating these 2D interpreted results into mine planning software. The use of this 2D dataset should be extended beyond the initial interpretation and mine planning stage. For example, the use of seismic cross sections and seam elevation data which have been derived from the seismic volume, may assist with optimising longwall production and help with in-seam drilling for gas drainage.

Experience has shown that recording 3D seismic data, and mapping seismic attributes for their lateral variability, will greatly improve the interpretation of structure and allow the identification of structures well below the seismic resolution limit. In addition, valuable geo-technical information such as roof/floor conditions and variability of the near seam stratigraphy may also be obtained through a detailed attribute examination. Serious consideration should be given to acquiring 3D seismic data in the event of continued exploration in the Adani Survey area.

Disclaimer

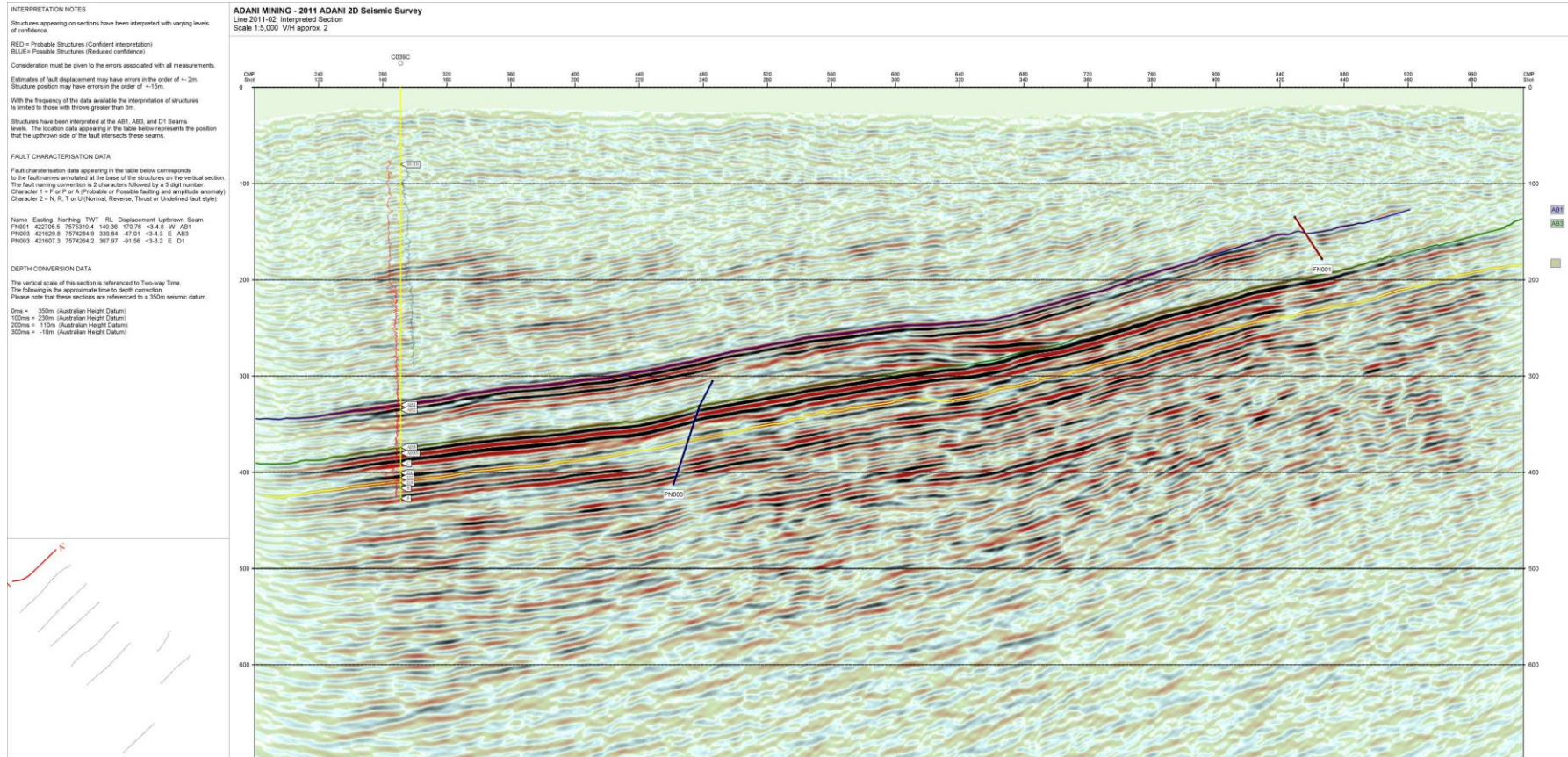
This report has been prepared in good faith and with all due care and diligence. It is based on the seismic and other geophysical data presented and referred to, in combination with the author's experience with the seismic technique, and as tempered by the geological and stratigraphic evidence presented in various forms and through discussions with client representatives.

As such, the report represents a collation of opinions, conclusions and recommendations, the majority of which remain untested at the time of preparation. In the light of these facts it must be clearly understood that Velseis Processing Pty Ltd and its proprietors and employees cannot take responsibility for any consequences arising from this report.

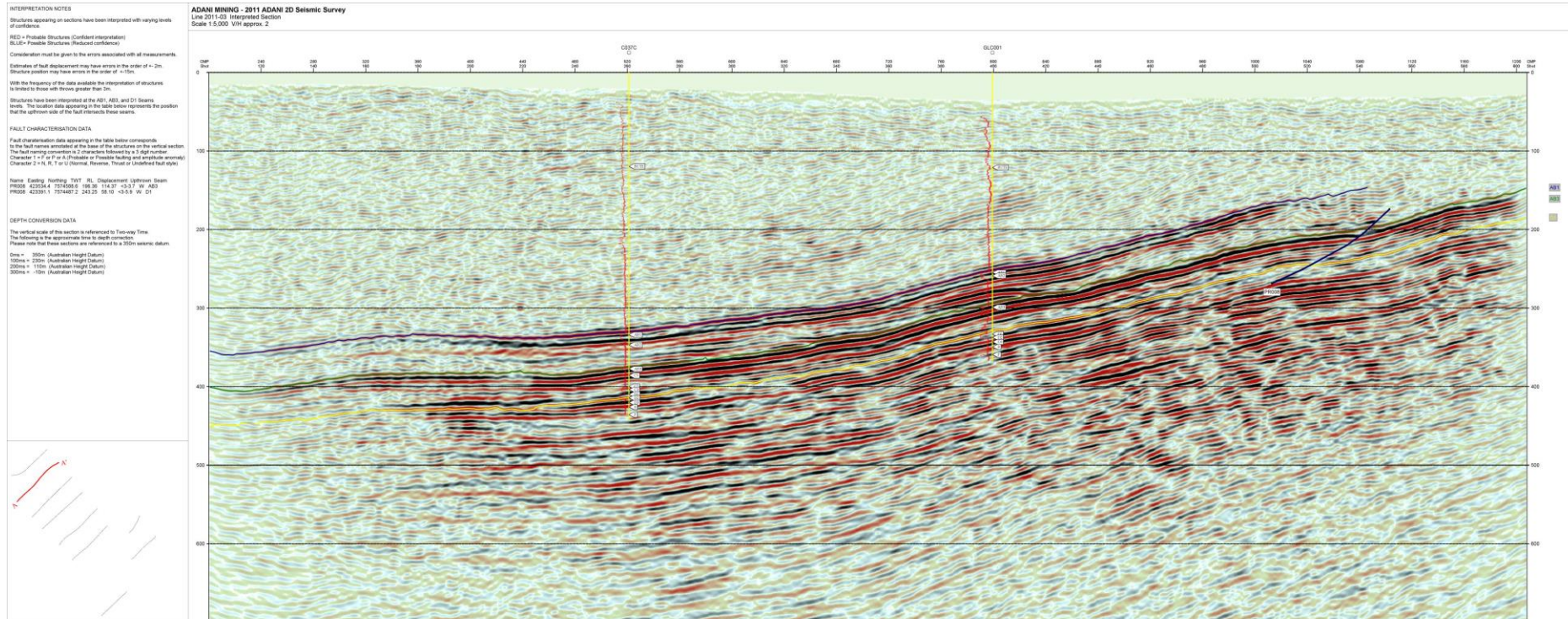
APPENDIX A SEISMIC SECTIONS

Interpreted sections of Filtered migrated stack with spectral enhancement.
Images displayed are not to scale.

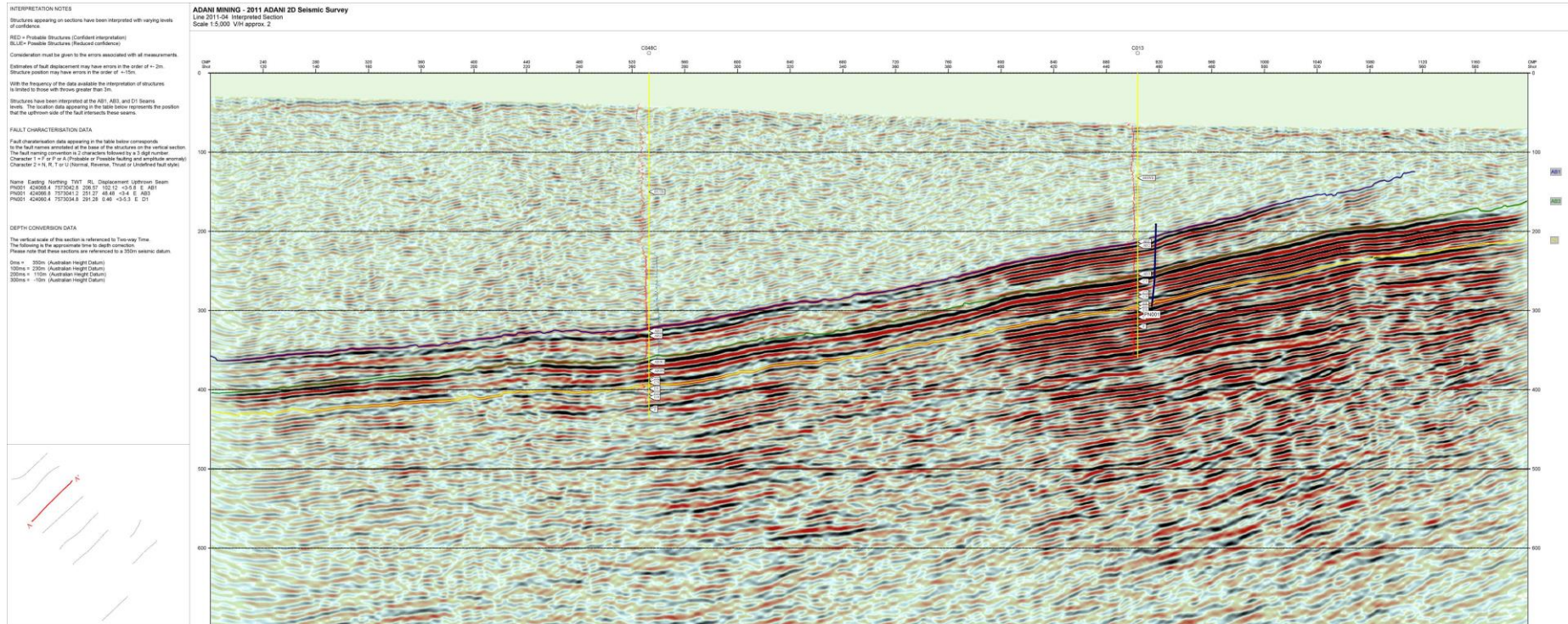
Line 2011-02



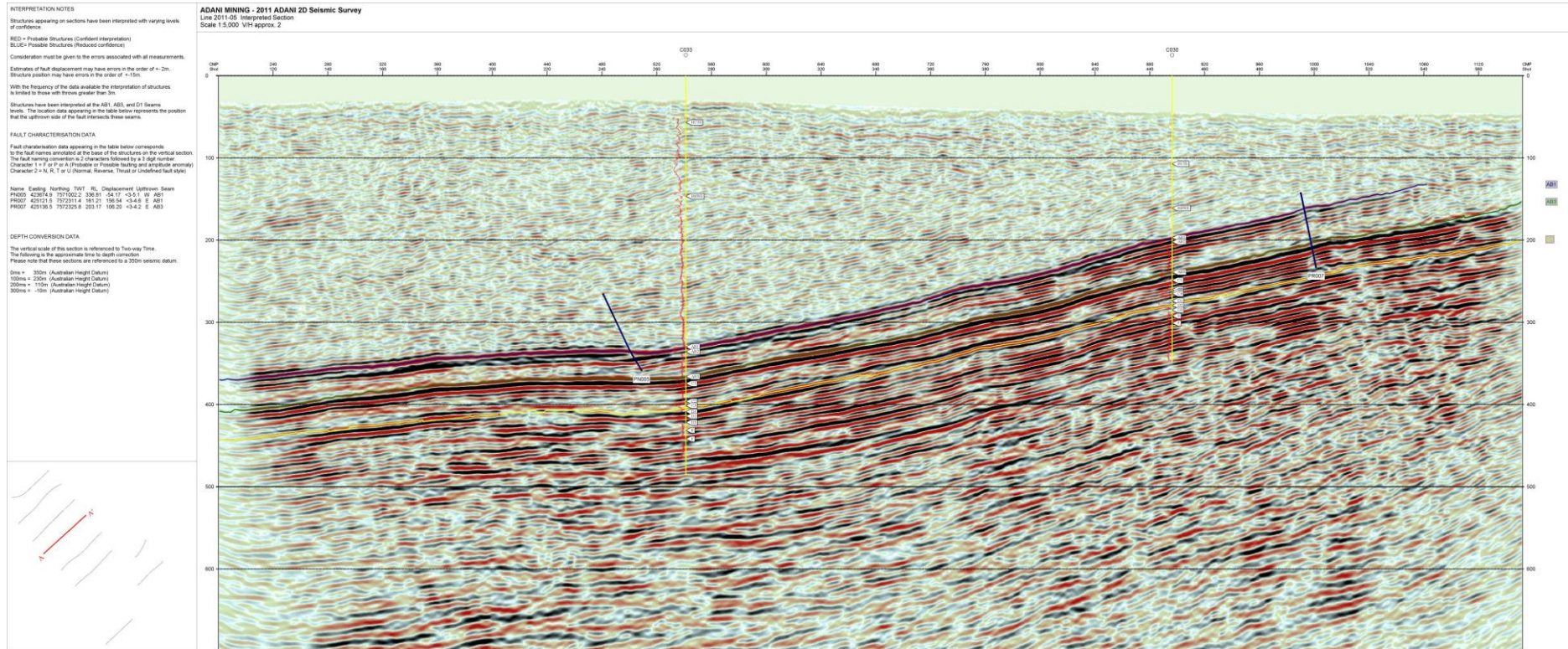
Line 2011-03



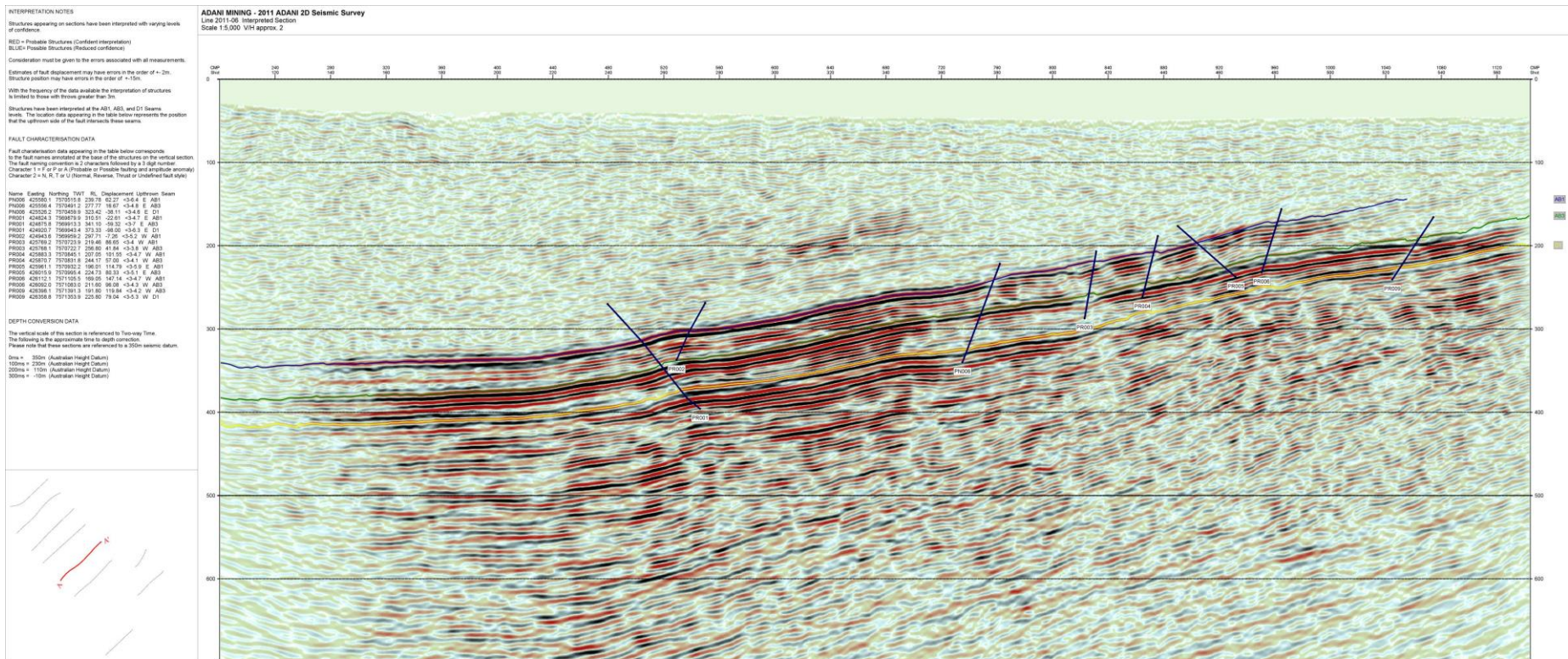
Line 2011-04



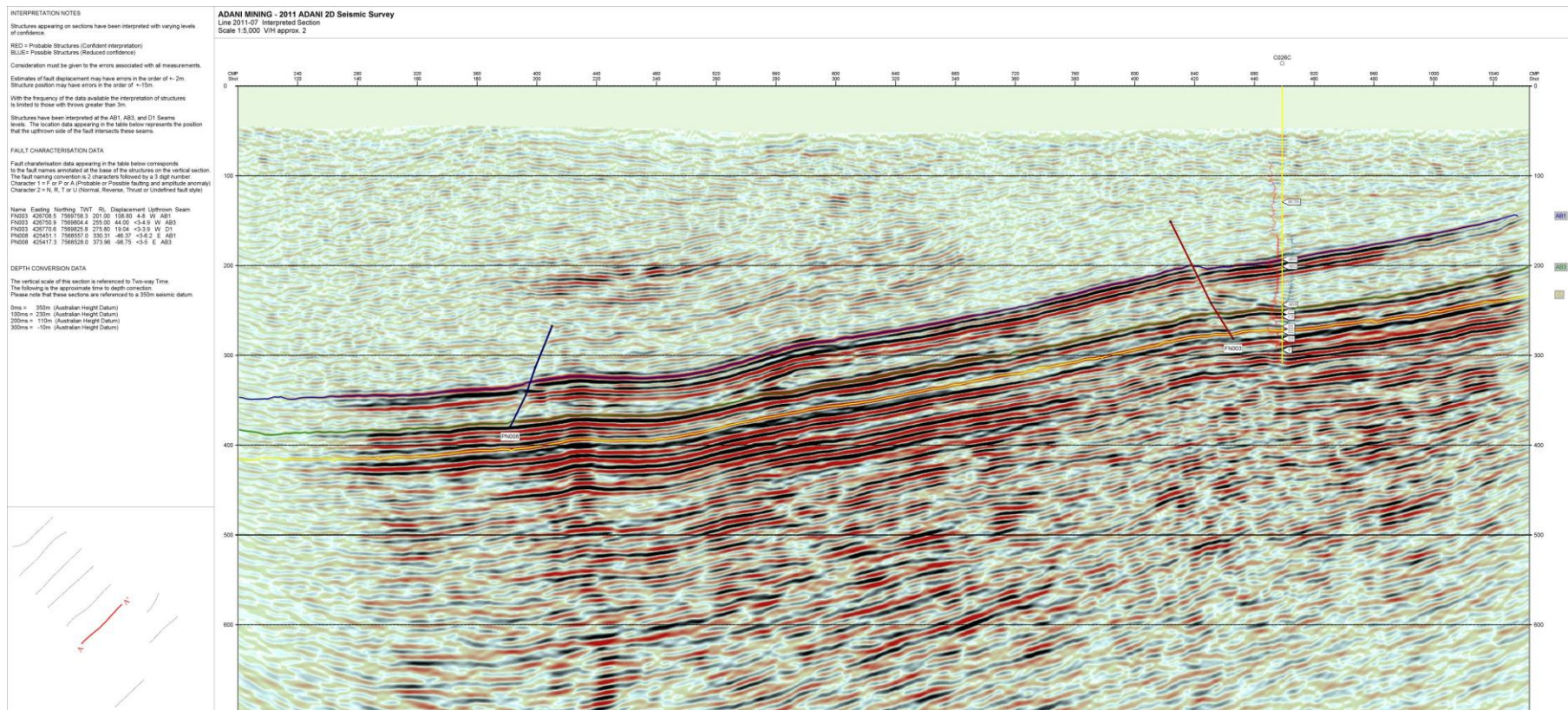
Line 2011-05



Line 2011-06



Line 2011-07



Line 2011-08

INTERPRETATION NOTES

Structures appearing on sections have been interpreted with varying levels of confidence.

RED = Probable Structures (Confident interpretation)
BLUE = Possible Structures (Reduced confidence)

Consideration must be given to the errors associated with all measurements.

Estimates of fault displacement may have errors in the order of $\pm 2\text{m}$.
Structure position may have errors in the order of $\pm 15\text{m}$.

With the frequency of the data available the interpretation of structures is limited to those with throws greater than 3m.

Structures have been interpreted at the AB1, AB3, and D1 Seams levels. The location data appearing in the table below represents the position that the upthrown side of the fault intersects these seams.

FAULT CHARACTERISATION DATA

Fault characterisation data appearing in the table below corresponds to the fault names annotated at the base of the structures on the vertical section. The fault naming convention is 2 characters followed by a 3 digit number. Character 1 = F or P or A (Probable or Possible faulting and amplitude anomaly) Character 2 = N, R, T or U (Normal, Reverse, Thrust or Undefined fault style)

Name	Easting	Northing	TWT	RL	Displacement	Uphrown	Seam
------	---------	----------	-----	----	--------------	---------	------

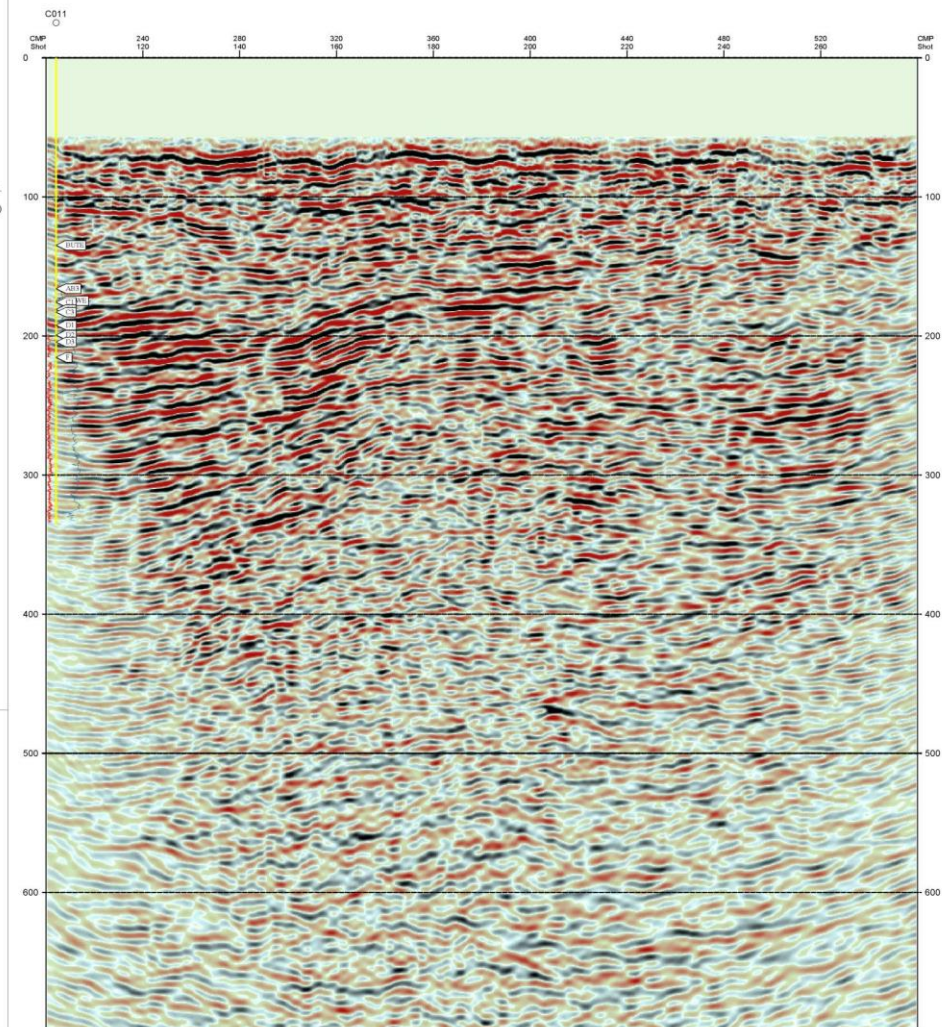
DEPTH CONVERSION DATA

The vertical scale of this section is referenced to Two-way Time.
The following is the approximate time to depth correction.
Please note that these sections are referenced to a 350m seismic datum.

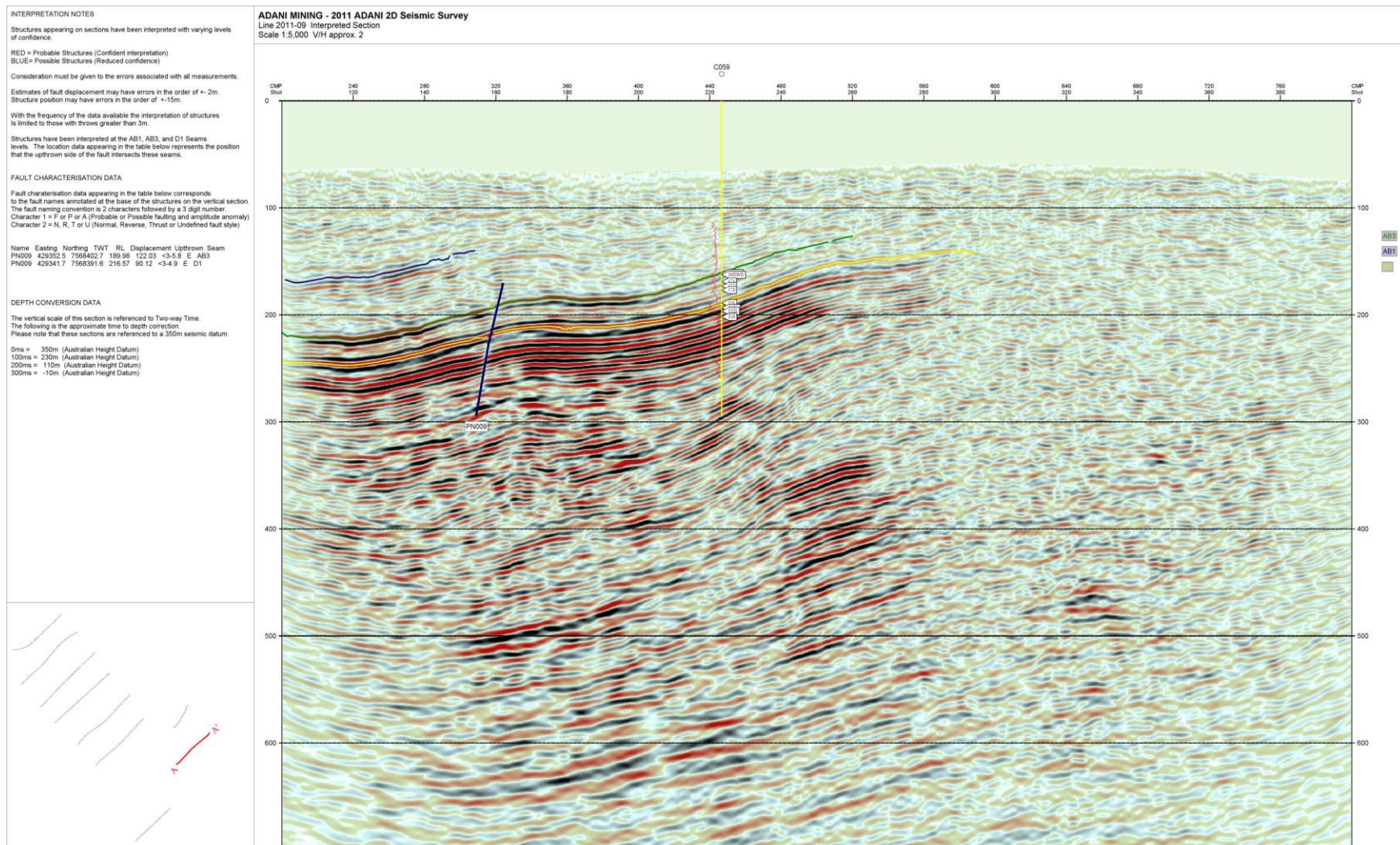
0ms = 350m (Australian Height Datum)
100ms = 230m (Australian Height Datum)
200ms = 110m (Australian Height Datum)
300ms = -10m (Australian Height Datum)

ADANI MINING - 2011 ADANI 2D Seismic Survey

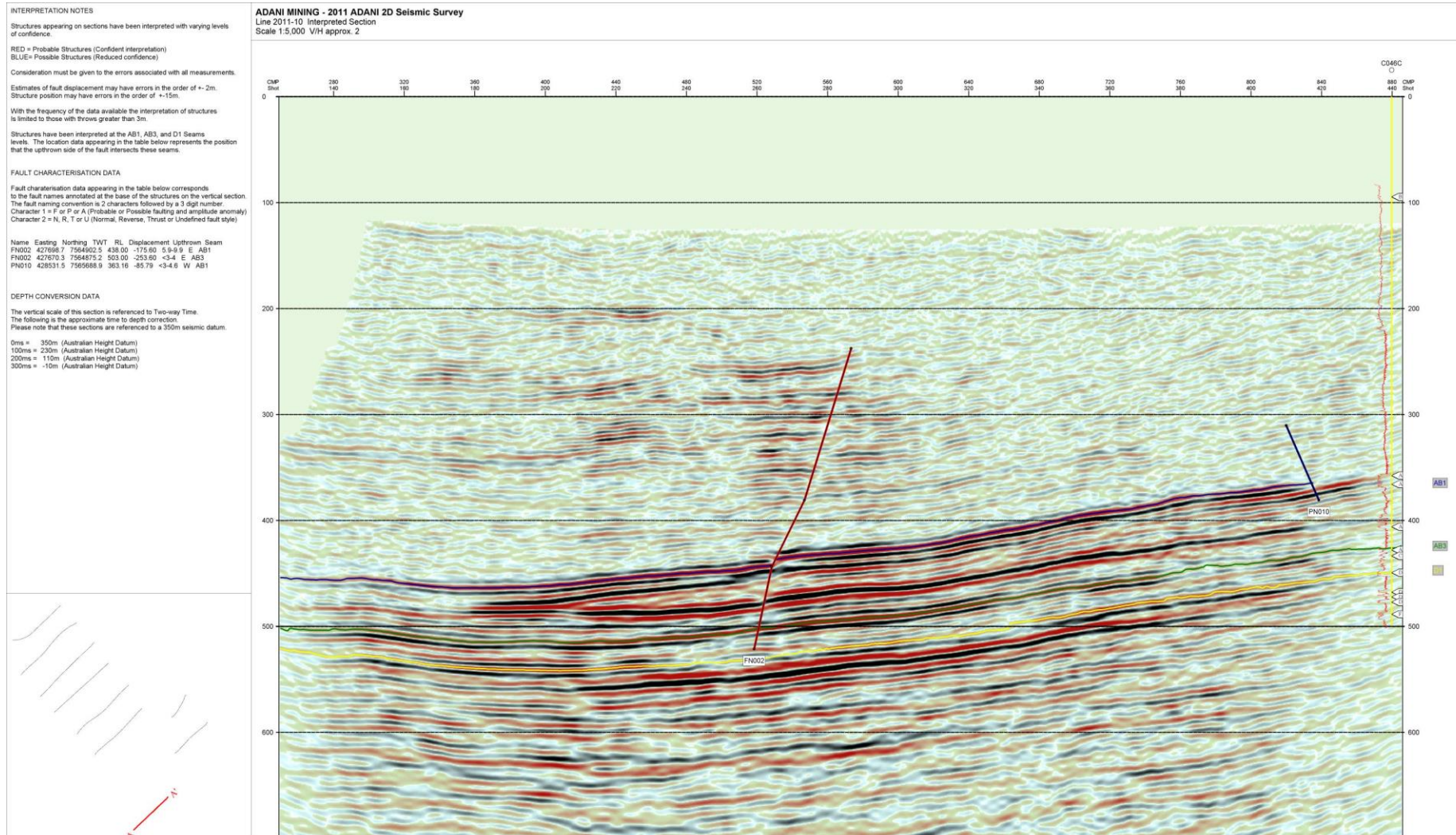
Line 2011-08 Interpreted Section
Scale 1:5,000 V/H approx. 2



Line 2011-09



Line 2011-10

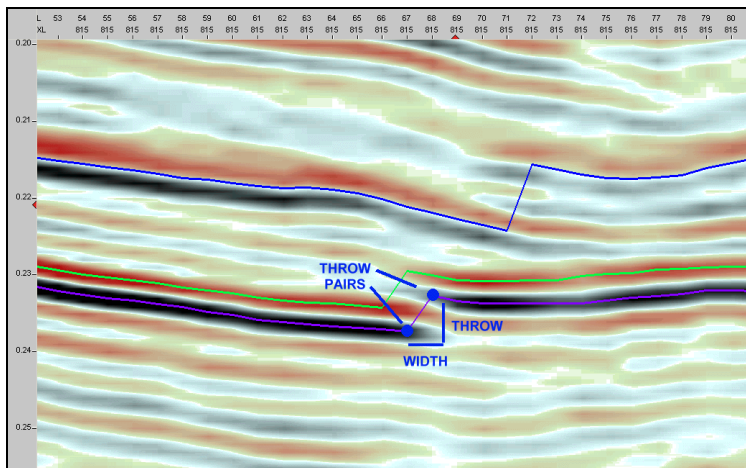


APPENDIX B Fault Methodology

The diagram below displays the methodology associated with the seismic displacement ('throw') and width calculation. The 'throw' point pairs are exported and each point contains two way time, x and y coordinates. Fault 'throws' are estimated using the change in time of the seam over the fault. An average velocity of 2400 m/s was used to convert this time to a fault 'throw'. The 2400 m/s velocity is a regional value derived from experience and assessment of downhole sonic logs and velocity maps from the area.

$$\text{'Throw'} = (\text{Change in seam time}/2) * 2400$$

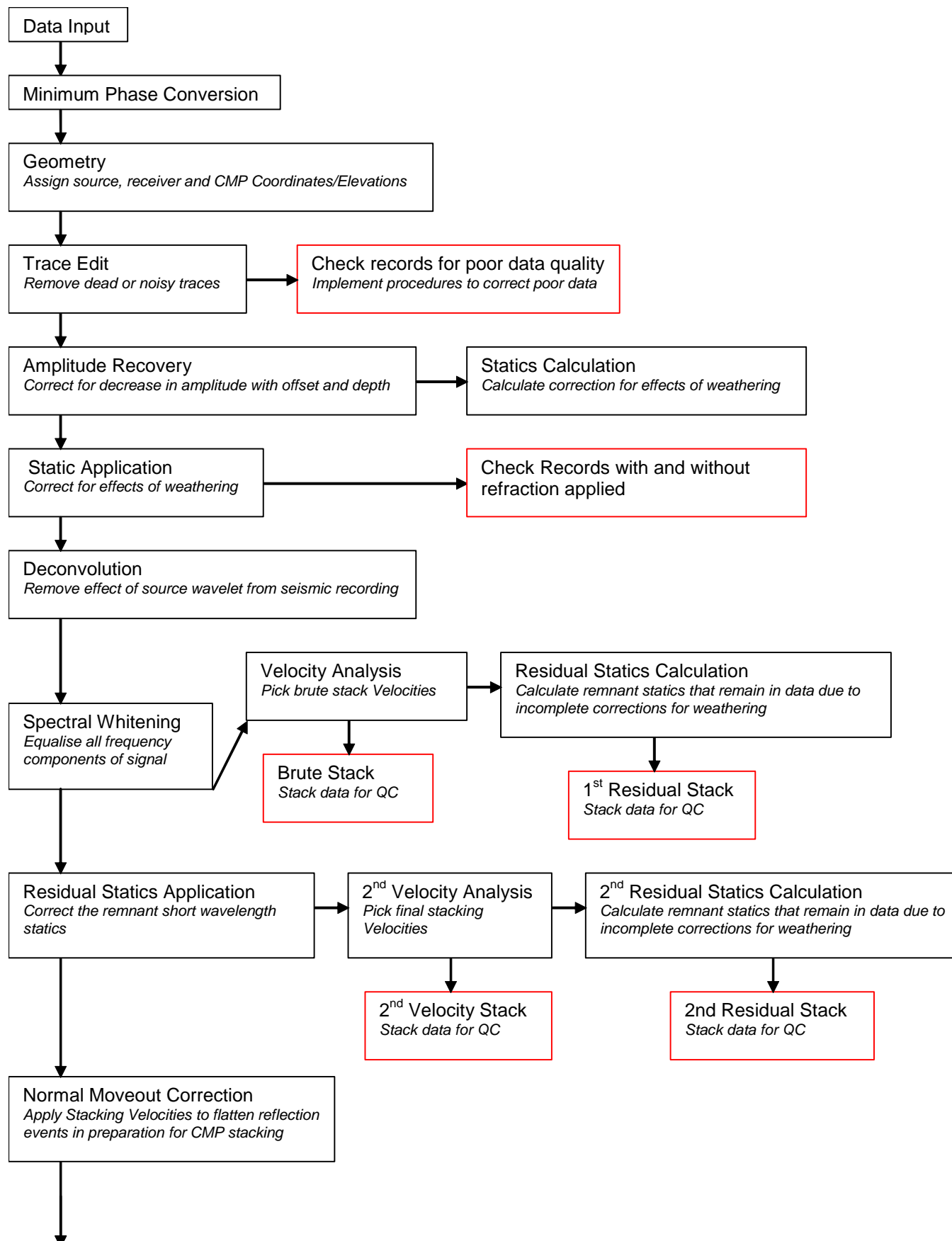
The fault width measurement is obtained by calculating the lateral change between the two fault 'throw' points.

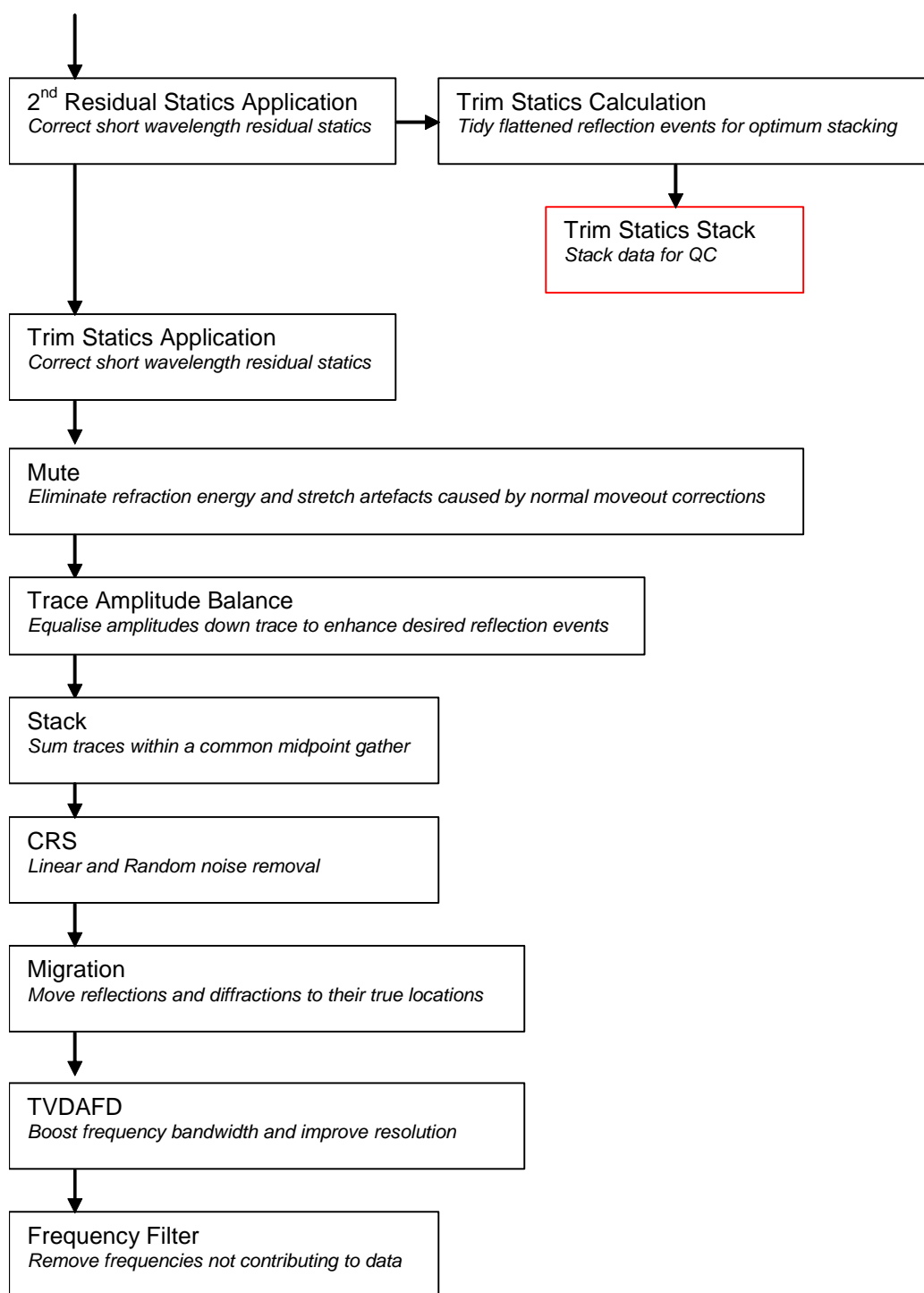


APPENDIX C PROCESSING

Processing Workflow

The Red boxes denote processing quality control points.





Processing System

The data were processed by VELSEIS PROCESSING PTY LTD.

VELSEIS PROCESSING uses ProMAX processing software. This is an interactive processing system allowing the user to view data processing at each stage, producing a final result of the highest quality.

The software executes on Velseis Processing's Linux cluster technology. The 48 node cluster is configured with eight core 1.8-3.2 GHz chips, 2-16 Gbyte memory communicating via a 1 Gbit network and provides significant improvements in processing speed. User interface is via X terminals networked to the main system. Each terminal has a high definition monitor to enable accurate representation of the digital data in pixel form.

Parameter Testing

The following processing parameters were tested:

Bandpass filter: Bottom cut frequency (shallow and deep)
Top cut frequency (shallow and deep)

Pre-stack F-K filtering: Whether or not to apply

NMO: Percentage stretch mute

AGC: Operator length

CRS: Post-stack aperture

DMO: Whether or not to apply

Common Offset F-X deconvolution: Whether or not to apply

Post-stack F-K Filter: Whether or not to apply

Migration: Percentage of smoothed velocities

Post-stack Noise attenuation: Whether to use Spectral whitening or TVDAFD
Frequency and exponential parameters

Processing Parameters

Reformat

Input data were reformatted from SEG Y to ProMAX internal data format.

Geometry

Geometry information was assigned to trace headers. Information assigned to each trace includes source, receiver and CDP locations, offsets, elevations and CDP fold.

Trace Edit

Dead or noisy traces were removed from shot records interactively and traces with reversed polarity were corrected.

Minimum Phase Filter

A filter was created to convert the data from zero phase to minimum phase.

Amplitude Recovery

Time and offset varying scalars were applied to traces to compensate for the effects of spherical divergence. The gain function applied at each sample is

$$G_{\text{amp}} = \frac{1}{T^2 V}$$

where T is the two-way time and V is the RMS Velocity

Static Computation and Application

Statics were calculated using a refraction static delay-time algorithm for all lines except Line 2011-10 where elevation statics were calculated. For the refraction static method first arrivals for a single refraction layer were initially picked. Shot and receiver delay times were then calculated using a least squares delay-time algorithm. Shot and receiver static corrections were then calculated using a constant surface-layer velocity (V_0) of 800 m/s. A replacement velocity of 2200 m/s and final datum of 350m was used for all lines.

The mean value of both the shot and receiver statics was applied to correct the data to a smoothed processing datum.

Deconvolution

Event resolution was enhanced using surface-consistent Spiking deconvolution. The deconvolution operators are obtained using the Wiener-Levinson algorithm. The surface-consistent approach assumes that the observed seismic wavelet results from filtering effects that include source, receiver, offset and CMP components.

The window for the deconvolution operator was designed to start after the first arrivals and finish at 450-700 ms dependant on offset. A spiking operator of 40ms in length and 0.01% white noise were created using the shot and receiver components.

Zero Phase Spectral Whitening

Zero Phase spectral whitening was applied post-stack to balance down ground roll and improve temporal resolution. The desired frequency range was divided into eight panels and balanced using a 125 ms sliding window.

Output Spectrum: 20-30-180-220 Hz

Velocity Analysis (1st Pass)

Velocities were picked using the ProMAX interactive velocity picking package (IVA) every 200m. IVA uses velocity spectra, moved out gathers and stacked panels to assist in a careful interpretation of stacking velocities. As the velocity function is altered, revised gathers and stacks are produced and reviewed until optimised stacking velocities are achieved.

Residual Static Calculation and Application (1st Pass)

Surface consistent residual statics were calculated and applied using Maximum Power Autostatics. Pilot or reference traces were formed using appropriate time gates by flattening traces along the Autostatics horizons and smashing several traces together.

Each trace from the active CDP is time shifted relative to the pilot trace and summed with it. The power of the stack is measured for each time shift. This shift-power trace is then summed with other traces having the same shot and receiver in their respective domains. After the shift spectra have been calculated for the entire line and summed in the receiver/shot domains, time shifts are picked at the maximum of the power shift spectra and stored as static values. The pilot stack is updated and the process repeated for a number of iterations.

Calculations were conducted for 5 iterations or until the RMS of the change in the computed static was less than .05ms. The maximum final static shift allowed was set to ± 10 ms.

Velocity Analysis (2nd Pass)

Following application of residual statics, second pass velocities were picked every 100m.

Residual Static Calculation and Application (2nd Pass)

To optimise shot and receiver residual statics, a second pass of surface consistent residual statics was applied following second pass velocity analysis. Pilot or reference traces were formed for appropriate time gates by flattening traces along the autostatics horizons and smashing several traces together.

In this case calculations were conducted for 5 iterations or until the RMS of the change in the computed static was less than .05ms. The maximum final static shift allowed was set to ± 10 ms.

Normal Moveout Correction

Hyperbolic normal moveout (NMO) was applied to the data using the following formula.

$$T_x^2 = T_0^2 + \frac{x^2}{v^2}$$

T_x = time at offset x

T_0 = time at zero offset

x = offset of the trace

v = stacking velocity at time T_0

Mute

A 30% stretch mute was applied to eliminate refractors and stretch caused by normal moveout corrections.

CDP Trim Statics

Non-surface consistent static shifts were calculated and applied after correlating each trace within a CDP with a pilot trace for that CDP. The pilot trace is the stacked trace of that CDP after F-X Deconvolution has been applied to the 2nd residual static stack. Shifts were limited to a maximum value of ± 4 ms. Trim statics were not applied to line 2011-08 as they did not improve the stack.

Trace Amplitude Balance (AGC)

AGC automatically varies the gain applied to trace samples within an AGC time window. The AGC scalar is based on the mean of the absolute values of the samples in the sliding time gate.

A scaling window of 100 ms was used.

Final Datum Shift

Gathers shifted from processing datum to final datum.

Stack

Traces within a common midpoint bin were summed. The post stack trace was scaled by the square root of the fold for each sample in the trace.

Common Reflection Surface Stack (CRS)

CRS uses dip and velocity information to create stacks of regularised CMP gathers with signal to noise improvements. A 12m post stack aperture has been used during this process.

Migration

All final stacks were migrated using a Steep Dip Explicit FD Time migration algorithm. This assumes a time varying and laterally variant smoothed velocity field. Migration used a smoothed version of the final stacking velocities. 110% of these velocities were used.

TVDAFD

TVDAFD was applied post-stack as a true amplitude, time varying form of spectral balancing. A 500ms sliding window with 50ms overlap was used, and the time-boost exponent functions applied were:

(time(ms) – exponent): 0-0.8 , 450-0.8 , 550-0.2 , 1000-0.2

Filter

Data were filtered for display using a zero phase, time variant Ormsby bandpass filter with the following corner frequencies:

0 – 400ms : 20-30-180-200 Hz
600 – 1000ms : 20-30-120-140 Hz

Quality Control

The following is a summary of the quality control steps taken throughout the processing of this data.

- Interactive display of all shot records for trace editing and geometry QC
- Geometry QC using Linear moveout, plus displays of trace offset, shot/receiver elevation, CDP fold, SP/CDP relationship
- Displays of stacks and corresponding CDP gathers
- Stack displays for refinement of stacking velocities, residual statics, filters, scaling and noise attenuation

Archive

DVD-769 containing:-

SEG Y data : Sample Rate 1ms, Data length 2000ms

Raw Migration

Filtered Migration

Filtered Migration with TVDAFD

Raw Stack

ASCII file :

Survey data

PDF file :

Processing report

APPENDIX D RESOLUTION OF SEISMIC INTERPRETATION

F.1 Vertical Resolution

There are a number of quasi-theoretical measures of vertical resolution, which are often used to determine the vertical resolving power of P-wave seismic data.

The 'detectable limit' is defined as the minimum layer thickness required to produce an observable seismic reflection (Sheriff, 1991). This is generally taken to be of the order of $\lambda_D/30$, where λ_D is the dominant wavelength of the P wave:

$$\lambda_D = \frac{V_{int}}{f_D}, \quad \text{F-1}$$

f_D is the dominant frequency of the seismic wave, and V_{int} is the interval velocity of the geological layer being considered. The dominant frequency in a seismic record is equivalent to $1/T$, where T is the time between adjacent peaks on a display of the seismic data (Figure F1). Note of course, that detection of a geological layer presupposes a sufficiently strong density and velocity contrast across the layer interfaces.

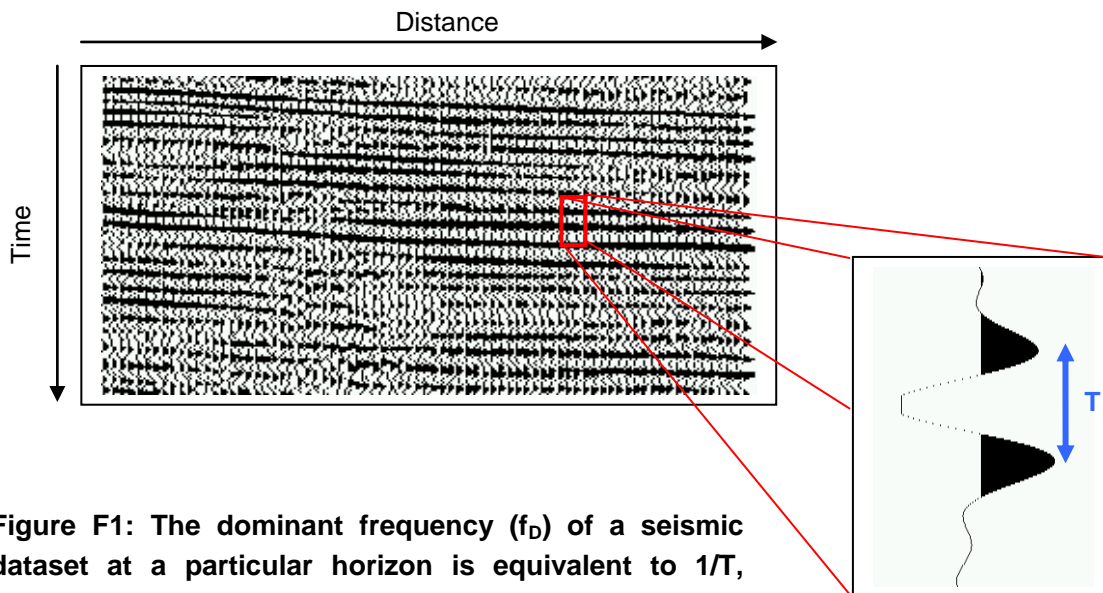


Figure F1: The dominant frequency (f_D) of a seismic dataset at a particular horizon is equivalent to $1/T$, where T is the time between adjacent peaks on the display of the seismic reflection event.

The commonly used 'Rayleigh resolution limit', defined as the minimum separation of discrete seismic reflectors at which one can ascertain more than one interface is present (Sheriff, 1991), is $\lambda_D/4$. The 'Widess limit' is an alternative, and more optimistic definition, which states that two interfaces are resolvable if their separation is greater than or equal to $\lambda_D/8$ (Sheriff, 1991).

Note that these rule-of-thumb measures for P-waves are approximate, and strictly derived for resolution issues relating to layer thickness. Nevertheless, they do provide some indication of the ability of a P-wave section to resolve other geological features (e.g. faults). Obviously these resolution measurements become over-optimistic in the presence of significant noise.

The average dominant frequency for the stacked P data across the target reflectors within the Adani survey is 100 Hz. The average P-wave interval velocity for the immediate coal seam roof is 2400m/s. Using equation

F-1, the dominant wavelength for the P-wave section is approximately 24 m. This implies that the Rayleigh resolution limit will be approximately 6 m and the Widess limit will be approximately 3 m. This suggests that, in theory, we should be able to characterise structures with displacements in the order of 3 m and greater.

F.2 Horizontal Resolution

For simplicity it is generally assumed that data recorded at a receiver is reflected from a point on a seismic layer. However, in reality a circular zone of data contributes to each reflection event recorded at each receiver (Figure F2) especially for unmigrated data. This zone of reflection is called the Fresnel zone, the size of which governs the horizontal accuracy of structural information that can be acquired from seismic data. The radius of the Fresnel zone is dependent on the reflection depth, frequency content and seismic velocity.

For a P wave the radius of the Fresnel zone (r_p) can be approximated by:

$$r_p = (z \lambda / 2)^{1/2} \quad \text{F-2}$$

where: z equals the depth and; λ is the wavelength which is given by the average P-wave velocity divided by the dominant frequency

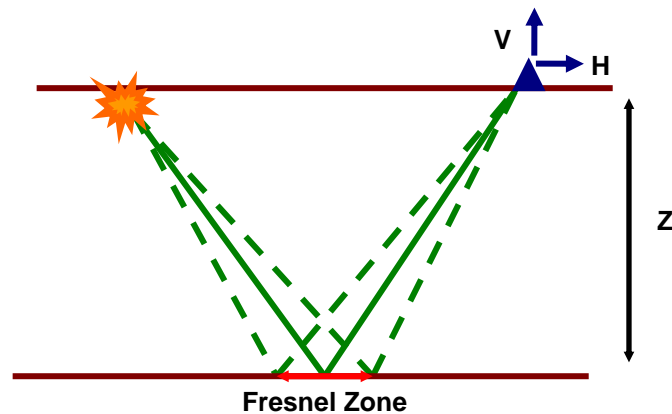


Figure F2. The horizontal resolution of seismic data is defined by the Fresnel zone. This is the reflection region for each shot and receiver pair.

Adani Data

Typical Fresnel zone radii for the survey area for a structure at a depth of 250m, assuming an average P-wave velocity of 2400m/s and dominant P wave frequency of 100Hz, would be 55 m. This horizontal resolution assumes that the seismic data are unmigrated. Therefore, the migrated P-wave data will have less error and based on the interpreters experience of previously validated data sets the lateral error of the migrated P-wave data for this survey may be up to 14 m.

APPENDIX E Glossary

This glossary contains explanations of technical terms and acronyms commonly used to describe seismic processing and interpretation. More comprehensive explanations can be found in standard seismic texts and reference books (e.g. Sheriff, R.E. (1991) Encyclopaedic Dictionary of Exploration Geophysics, Society of Exploration Geophysicists, Oklahoma).

2D	two-dimensional
2D	three-dimensional
AGC	automatic gain control; data-dependent scaling designed to normalise trace amplitude within a running time window
anisotropy	variation of seismic velocity depending on the direction in which it is measured; a sequence of sedimentary bedding produces polar anisotropy (where seismic velocities are symmetric about the bedding); non-horizontal fracturing and microcracks produces azimuthal anisotropy (where seismic velocities are symmetric about the axis perpendicular to the fracturing)
bandpass filtering	attenuation of seismic energy outside of a user-defined frequency bandwidth
CMP stacking	the summation of all traces within a CMP gather
common midpoint (CMP) gather	the set of seismic traces that share the same midpoint between their sources and receivers
common receiver gather (CRG)	a collection of seismic traces recorded at the same geophone (receiver) location
deconvolution	a process designed to restore a waveshape to the form it had before undergoing a filtering action; applied to seismic reflection data to remove the filtering effect of the earth and so improve the resolution of reflected energy
dominant frequency	the predominant frequency of a seismic dataset determined by measuring the time between successive peaks or troughs of the recorded seismic pulse, and taking the reciprocal
fold	the multiplicity of data within a CMP gather; that is, the number of traces within a CMP gather that will contribute to the summed trace at that CMP location
dominant wavelength	the seismic wavelength associated with the dominant frequency; for P waves, equivalent to V_p divided by the dominant frequency
frequency	the repetition rate of a periodic waveform, measured in 'cycles per second' or Hertz (Hz)
frequency bandwidth	range of frequencies over which the recorded seismic signal has significant power
f-xy deconvolution	a random-noise attenuation method typically applied to seismic data following CMP stacking; improves the signal-to-noise ratio of the final stack
geometric spreading	see spherical divergence

geophone	the recording device or receiver used to transform seismic energy into an electrical voltage for input into the seismic recording system; a single vertically-oriented geophone is used for conventional seismic acquisition
geophone array	a group of geophones arranged in a linear or areal pattern connected to a single recording channel (i.e. the ground motion recorded by each of the geophones within the array is summed to produce just one seismic recording at the particular receiver station); used to discriminate against waves with certain dominant wavelengths and boost the signal-to-noise ratio
geophone array length	the distance over which a geophone (receiver) array is planted about a receiver station; typically of the order of 20-30m for petroleum-scale recording and 2-5m for coal-scale seismic recording
groundroll	a type of seismic wave that travels along or near the surface of the ground; characterised by relatively low velocity, low frequency and high amplitude; recorded as a steeply dipping, linear event on a seismic shot record; often interferes with desired reflection events
instantaneous frequency attribute	the temporal rate of change of the instantaneous phase; generally has a high degree of variation that can often be related to stratigraphy
instantaneous phase attribute	a measure of the lateral continuity of events on a seismic section
magnitude spectrum	amplitude of seismic recording as a function of frequency
migration	a seismic inversion operation involving rearrangement of seismic data samples so that reflections are plotted at their true locations; required where laterally varying seismic velocities and dipping reflectors cause seismic energy to be recorded at relative positions different to their real physical location
mute	elimination of unwanted energy from seismic traces; typically used over certain time intervals to remove groundroll or noise bursts out of the final stack
normal moveout (NMO)	the variation of the arrival time of reflection energy with offset; NMO corrections compensate for this variation in traveltime so that reflection energy from each geological boundary is properly aligned prior to stacking; for horizontal reflectors, P-wave NMO can be described as hyperbolic
offset	the distance from the source point to the receiver location
P waves	longitudinal or compressional seismic waves; characterised by particle motion in the direction of travel; acquired using conventional (single-component) seismic acquisition surveys
predictive deconvolution	a method of deconvolution that takes advantage of the predictability of surface multiples; provided necessary statistical assumptions are met, predictive deconvolution will remove surface multiple energy at the same time as removing the filtering effect of the earth to produce high resolution seismic reflection events

receiver array	see geophone array
reflection amplitude attribute	a measure of the amplitude of seismic energy reflected from a specific geological interface; instantaneous amplitude is the amplitude recorded at the interpreted arrival time of the seismic event; RMS amplitude is the root-mean-square amplitude determined over a window of a specified length centred about the interpreted arrival time of the seismic event
reflection gradient attribute	a measure of the rate of variation in arrival time of a seismic event; anomalously high gradients are generally indicative of structures or rapidly varying depths of the reflector being analysed
residual static corrections	remnant statics associated with incomplete weathering static corrections
resolution	the ability to separate two features which are very close together
resolution limit	for discrete seismic reflectors, the minimum vertical separation so that one can ascertain that more than one interface is involved; the commonly used Rayleigh resolution limit is defined as one quarter the dominant wavelength; the Widess limit is defined as one eighth the dominant wavelength
S waves	transverse or shear seismic waves; characterised by particle motion perpendicular to the direction of travel; acquired using multi-component (3-C) seismic acquisition
seismic attribute	typically refers to some measurement extracted from seismic data beyond conventional reflection two-way time (TWT); typically presented as an auxiliary 2D surface or image; commonly used attributes include reflection amplitude, instantaneous frequency or reflection gradient (dip) (see independent entries for a description of these attributes)
seismic waves	sound waves that propagate through the earth
seismic modelling	generation of a synthetic seismic record given an earth model
seismic reflection	a geophysical method to image the sub-surface using artificially-generated sound waves; typically the arrival times of various seismic waves are used to map sub-surface structure
seismic source	an artificial device that releases energy or seismic waves into the ground; typical coal-seismic sources include small dynamite explosions, MiniSOSIE and Vibroseis
seismic velocity	the propagation speed of a seismic wave through a particular material
shot record	a collection of seismic traces recorded at a number of receivers from the release of seismic energy at a single source location
signal-to-noise ratio (S/N)	the ratio of desired signal to all other recorded energy (noise) in a seismic recording; may be difficult to determine in practice
spectral whitening	a signal processing procedure whereby all frequency components within a signal bandwidth of a seismic recording are equalised
spherical divergence	the decrease in seismic wave strength with distance; caused by seismic waves continually spreading out as they travel through a medium so that energy density decreases

spherical divergence correction	a scaling correction to compensate for decrease in wave strength with distance as a result of geometric spreading
stacking	process by which a set of seismic traces are summed
static corrections	corrective time shifts applied to seismic data to compensate for the effects of variations in elevation, weathering thickness, weathering velocity or reference to datum; the objective is to determine the arrival times which would have been observed if all measurements had been made on a flat plane with no weathering or low-velocity material present
structural interpretation	involves the mapping of geological interfaces and discontinuities (such as faults) via picking of the TWT of seismic reflection energy from target reflectors
trim statics	corrective time shifts applied to NMO-corrected CMP gathers prior to stacking; designed to optimally align flattened reflection events
TWT	two-way traveltime; refers to the time it takes for seismic energy to travel from the seismic source, down to a reflector, and back to the surface receiver
velocity analysis	calculation of a velocity that will accurately compensate for the effects of NMO; typically involves flattening reflection events in a CMP
wavelength	the distance (in metres) between two successive similar points on two adjacent cycles of a seismic wave, measured perpendicular to the wave front; often represented by the symbol λ